STUDY OF BUCK–BOOST CONVERTER USING STATE SPACE ANALYSIS TECHNIQUE

A Thesis Submitted

in Partial Fulfilment of the Requirements

for the Degree of

MASTER OF TECHNOLOGY

By

Lt Prasad M Moghe

to the

DEPARTMENT OF ELECTRICAL ENGINEERING

INDIAN INSTITUTE OF TECHNOLOGY KANPUR

MARCH, 1996

EE-1996-M-MOG-STU

Certificate

It is certified that the work contained in the thesis entitled **STUDY OF BUCK–BOOST CONVERTER USING STATE SPACE TECHNIQUE** by *Lt. Prasad M Moghe* has been carried out under my supervision and that this work has not been submitted elsewhere for a degree.

(Dr.A Joshi)
Professor
Department of Electrical Engineering
Indian Institute of Technology
Kanpur-208016 India

February, 1996.

Acknowledgement

I would take this opportunity to express my sincere gratitude towards Dr A Joshi, my thesis supervisor for his invaluable guidance. I would also like to thank Mr R K Singh, Mr K Mahapatra, and Mr Hemant Agarawal for rendering me valuable suggesstions during my work.

With a sense of special regard I would like to express my indebtedness to Dr S C Srivastava, for providing his lab facilities to me. It was a great support during my thesis.

I thank Sqd Ldr A J Devakumar, Lt. M Puri and Lt S K Shrivastav, who were a great support during my thesis preparation.

Finally, I would like to express my gratitude towards the Indian Navy for having given me this opportunity.

Lieutenant Prasad Moghe

Abstract

The *state space analysis technique* is employed to investigate the dc-to-dc *Buck-Boost Converter*. This technique reveals two distinct families of state trajectory. The use of these state trajectories, for studying the dc-to-dc power converters has been shown to be a valuable method for analysis. A method has been proposed to simulate the state trajectories and find their intersection. The analysis carried out with these trajectories results in performance curves of the converter. The normalized performance curves have been obtained, which can be used for variety of converter operations. Further a design example based on these performance curves has been given. Finally the converter operation under three different control strategies has been studied. Also the computer simulated response of controllers based on these strategies has been presented.

Contents

List of Figures

Chapter 1

Introduction

The power converters and inverters are major building blocks in modern power electronics equipments. These systems are highly nonlinear in nature and are often classified as 'switched' linear system. In recent years increasingly more attention has been given to analysing, simulating and understanding principle of operation of these systems. In this respect the variety of mathematical analysis and computer simulation techniques are available for quantitative analysis.

However, in addition to the detail quantitative analysis, it is often useful to examine a nonlinear system in a qualitative manner. This enables the conceptual visualization of system nonlinearities. One such approach to study the switched linear system which enables a useful visualization of overall system behaviour is *state space approach.* This approach can reveal the qualitative insight into fundamental nature of the operation of system. It is also an effective tool to study the behaviour of the system, both in steady state and transient condition. In this thesis, the Buck- Boost converter will be considered, to study and illustrate the concept of this technique.

1.1 Scope of the Thesis

The basic Buck–Boost converter has two distinct modes of operation for continuous current conduction operation. These modes depend upon the state of switch(S) and diode(D). The normal method of analysis involves the solution of differential equations of these modes in time domain. However, the resulting time domain analysis can not provide the design information. Therefore the state space analysis method has been used. The procedure involved in analysis of the converter using state space technique can be broadly described as follows

A) *Development of state space representation of converter system.*

The basis of state space analysis is the portrait of a converter system in state space. The state space representation of converter operation results in the two distinct families of curves which are generally known as *system state trajectories.* The understanding of these trajectories and knowing how they vary with changes in system parameters and externally imposed operating conditions reveals certain fundamental characteristics of converter system. The values of inductor current($I_{Ln}(0)$) and capacitor voltage($V_{Cn}(0)$) have been used to generate family of state trajectory in these two modes.

B) *Analysis of steady state behaviour of converter*

The analysis of the converter has been carried out with the help of these families of state trajectory. During steady state operation, the system state traverses a closed loop consisting of one trajectory corresponding to each mode of operation. Hence the analysis of converter requires the study of intersection of two families of state trajectory. A method has been proposed to simulate the state trajectories and find their intersection. The performance curve for the entire range of converter operation has been obtained from the result of the above method. This approch enables one to examine the relative merits and demerits of various operating conditions. The comparative study carried over entire range of operation can be utilized for successful design of converter

system

With these performance curves, converter operations under diffrent operating conditions can be visualized. In addition, the ability of state space representation to observe the movement of the system state is the key factor in transient study of converter. This can reveal the complete understanding of the manner in which various control techniques accomplish their task. Hence the theoratical insight gained through this analysis can be used to postulate various control strategies which will improve the system performence.

1.2 Organization of the Thesis

The basic circuit used for this purpose has been introduced in Chapter 2. In sections 2.2 to 2.4, the converter has been represented by a state equation model and the time domain analysis has been studied. The sections 2 5 & 2.6 contain the

state space analysis of the converter.

In Chapter 3, various algorithms used for analysis of steady state behaviour of converter have been discussed. The performance curves obtained from the detailed analysis have been presented in section 3.2. A design procedure based on the performance curves has been proposed in section 3.3.

The operations of the converter under three control strategies have been simulated in Chapter 4. These strategies are

1. Input current limit and output voltage limit control

2. Stored energy level control

3. Trajectory law control

Chapter 2

State Space Analysis of Converter

In study of DC–DC converter, state space approach can be an effective tool for indepth analysis, as well as it can reveal a better qualitative insight of converter operation. The basis of this approach is the representation of converter on a state space. For the conceptual development of this study technique, a Buck–Boost DC–DC converter can be selected.

Section 2.1 describes the basic converter model and different modes of operation. In section 2.2, the converter has been represented by differential equation model (i. e. the state equation model) in different modes of operation. The normalization scheme for these state equations is discussed in section 2.3. The time domain representation of the converter system is given in section 2.4. This section also presents a method for simulation of the converter operation in time domain. The representation of the converter system in the state space is explained in section 2.5 along with the derivation of the equations of the state trajectories. Finally, the various features of the state trajectories are discussed in section 2.6.

2.1 The Basic Converter

The schematic diagram of Buck–Boost converter is presented in figure 2.1, where the effective series resistance of inductor(L) and capacitor(C) are shown by r_L and

r_C, respectively. The switch(S) and diode(D) are assumed to be ideal.

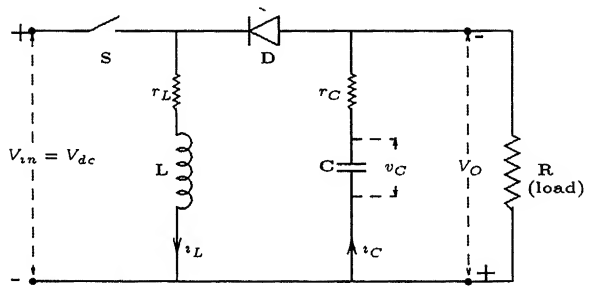

Figure 2.1: A basic buck-boost converter

2.1.1 Different Modes of Converter Operation

Due to the presence of the switching element(S), the converter is a discrete system. It has three different modes of operation such as:-

- Mode–1 :- S_{ON} and D_{OFF}
- Mode–2 :- S_{OFF} and D_{ON}
- Mode–3 :- S_{OFF} and D_{OFF}

The converter can be analysed as a system of three different circuits, corresponding to each mode. Figure 2.2 shows the equivalent circuit of the converter in these modes.

During operation with continuous inductor current, one cycle of operation consists of mode–1 followed by mode–2. In discontinuous inductor current conduction, one cycle of operation is, mode–1 followed by mode–2 and then by mode–3.

2.2 State Equation Model of Converter

The converter behaviour (i. e. instantaneous state of the converter) can be described with the help of three sets of differential equations formed by applying KCL and

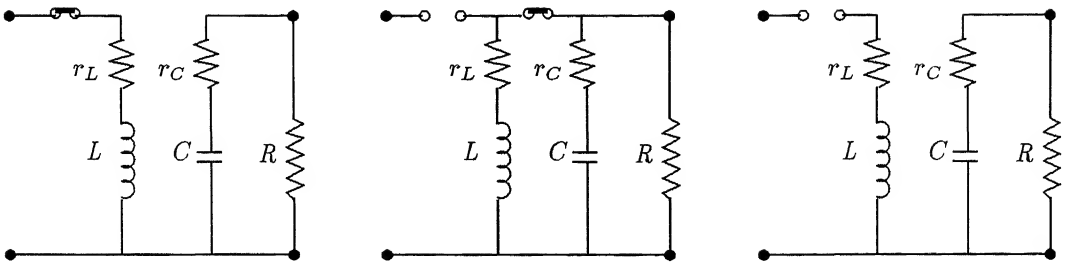

Figure 2.2: Equivalent circuit in different modes of converter operation

KVL to the equivalent circuits shown in figure 2.2. Thus, by choosing the *inductor current* and *capacitor voltage* as *state variables*, the state equations for the converter can be written as follows.

Mode–1 (S_{ON} **and** D_{OFF})

$$\frac{dv_C}{dt} = -\frac{v_C}{(R+r_C)C} \tag{2.1}$$

$$\frac{di_L}{dt} = \frac{V_{dc}}{L} - \frac{r_L}{L} i_L \tag{2.2}$$

Mode–2 (S_{OFF} **and** D_{ON})

$$\frac{dv_C}{dt} = -\frac{v_C}{(R+r_C)C} + \frac{R}{C(R+r_C)} i_L \tag{2.3}$$

$$\frac{di_L}{dt} = -\frac{v_C}{L} - \frac{r_L}{L} i_L \tag{2.4}$$

Mode–3 (S_{OFF} **and** D_{OFF})

$$\frac{dv_C}{dt} = -\frac{v_C}{(R+r_C)C} \tag{2.5}$$

$$i_L = 0 \tag{2.6}$$

2.3 Normalization Scheme for State Equations of Converter

The state equations 2.1 to 2.6 have to be normalized for the purpose of generality and to facilitate relative comparison. The selection of various normalization factors (base quantities) will be done by considering the quantities such as, voltage drop accross the inductor, the current through the capacitor and output voltage. The normalization of these quantities can be carried out as shown below The symbols used with subscript 'n' and 'b' are used to denote the normalized and base quantities of the corresponding variables, respectively.

- *Normalized voltage accross the inductor* is given as

$$\begin{aligned} v_{Ln} &= \frac{v_L}{V_b} \\ &= \frac{L}{V_b} \cdot \frac{di_L}{dt} \end{aligned} \tag{2.7}$$

Let the Base impedance(Z_b) be defined as $\frac{V_b}{I_b}$.

Therefore equation 2.7 can be written as

$$\begin{aligned} v_{Ln} &= \frac{L}{Z_b I_b} \cdot \frac{di_L}{dt} \\ &= \frac{L}{Z_b} \cdot \frac{d}{dt}\left(\frac{i_L}{I_b}\right) \\ &= \frac{L}{Z_b} \cdot \frac{di_{Ln}}{dt} \end{aligned} \tag{2.8}$$

Let time 't' be normalized as $t_n = \frac{t}{t_b}$

Therefore equation 2.8 can be written as

$$\begin{aligned} v_{Ln} &= \frac{L}{Z_b} \cdot \frac{di_{Ln}}{dt_n}\frac{dt_n}{dt} \\ &= \frac{L}{Z_b t_b} \cdot \frac{di_{Ln}}{dt_n} \end{aligned} \tag{2.9}$$

Let us define the *normalized inductor* as

$$L_n = \frac{L}{Z_b t_b} \tag{2.10}$$

From equations 2.9 & 2.10 we can write

$$v_{Ln} = L_n \cdot \frac{di_{Ln}}{dt_n} \tag{2.11}$$

- Similarly *Normalized current through the capacitor* is given as

$$i_{Cn} = C_n \cdot \frac{dv_{Cn}}{dt_n} \tag{2.12}$$

Where the *normalized capacitor*(C_n) is defined as

$$C_n = \frac{C Z_b}{t_b} \tag{2.13}$$

- And the *Normalized output voltage* is given as

$$v_{On} = R_n i_{On} \tag{2.14}$$

Where the *normalized load resistance* R_n is defined as

$$R_n = \frac{R}{Z_b} = R\sqrt{\frac{C}{L}} \tag{2.15}$$

The normalization scheme is chosen such that *values of normalized input voltage, normalized inductor and normalized capacitor are unity and normalized time of* 2π *corresponds to undamped natural period of inductor-capacitor combination.*

This leads to the various normalization factors (base quantities) as follows :-

- Base Voltage (V_b) = V_{dc}
- Base Current (I_b) = $V_{dc}\sqrt{\frac{C}{L}}$
- Base impedance (Z_b) = $\sqrt{\frac{L}{C}}$

- Base time $(t_b) = \sqrt{LC}$

Thus the normalization of the state equations 2.1 to 2.6 would result into the equations given below.

Mode–1 (S_{ON} **and** D_{OFF})

$$\frac{dv_{Cn}}{dt_n} = -\frac{1}{(R_n + r_{Cn})} v_{Cn} \quad (2\ 16)$$

$$\frac{di_{Ln}}{dt_n} = 1 - r_{Ln} i_{Ln} \quad (2.17)$$

Where

$$r_{Cn} = \frac{r_C}{Z_b}$$

$$\& \quad r_{Ln} = \frac{r_L}{Z_b}$$

Mode–2 (S_{OFF} **and** D_{ON})

$$\frac{dv_{Cn}}{dt_n} = -\frac{v_{Cn}}{R_n} + \frac{R_n}{(R_n + r_{Cn})} i_{Ln} \quad (2.18)$$

$$\frac{di_{Ln}}{dt_n} = -v_{Cn} - r_{Ln} i_{Ln} \quad (2.19)$$

Mode–3 (S_{OFF} **and** D_{OFF})

$$\frac{dv_{Cn}}{dt_n} = -\frac{1}{(R_n + r_{Cn})} v_{Cn} \quad (2.20)$$

$$i_{Ln} = 0 \quad (2.21)$$

The effective series resistances of inductor and capacitor can be neglected for the sake of simplicity and convenience of treatement. However, it should be noted that the validity of theoretical treatment developed does not depend upon nature of the component and can be extended to converter of arbitrary complexity. With this approximation, the equations 2.16 to 2.21 can be written as given below.

Mode–1 (S_{ON} **and** D_{OFF})

$$\frac{dv_{Cn}}{dt_n} = -\frac{v_{Cn}}{R_n} \tag{2.22}$$

$$\frac{di_{Ln}}{dt_n} = 1 \tag{2.23}$$

Mode–2 (S_{OFF} **and** D_{ON})

$$\frac{dv_{Cn}}{dt_n} = -\frac{v_{Cn}}{R_n} + i_{Ln} \tag{2.24}$$

$$\frac{di_{Ln}}{dt_n} = -v_{Cn} \tag{2.25}$$

Mode–3 (S_{OFF} **and** D_{OFF})

$$\frac{dv_{Cn}}{dt_n} = -\frac{v_{Cn}}{R_n} \tag{2 26}$$

$$i_L = 0 \tag{2.27}$$

2.4 Time Domain Solution of The Converter

The solution of these state equations would yield a *time domain solution* of circuit variables v_{Cn} and i_{Ln} as given below.

Mode–1(S_{ON} **and** D_{OFF})

$$v_{Cn} = (v^0_{Cn})_{on} e^{-\frac{t_n}{R_n}} \tag{2.28}$$

$$i_{Ln} = (i^0_{Ln})_{on} + t_n \tag{2.29}$$

Where

$(v^0_{Cn})_{on}$ and $(i^0_{Ln})_{on}$ are initial conditions of v_{Cn} and i_{Ln} ,

at the start of mode–1, respectively

Mode–2 (S_{OFF} **and** D_{ON}) The time domain solution in this mode has one of the three forms depending upon the value of per-unit load resistance(R_n) as given below. The detaialed solution and the calculation of constants A_v, B_v, A_i, B_i is given in appendix A. These constants are defined in terms of initial conditions of v_{Cn} and i_{Ln} at the start of mode–2 (*i. e.* $(v^0_{Cn})_{off}$ and$(i^0_{Ln})_{off}$ respectively).

- *For* $R_n < 1/2$

$$v_{Cn} = A_v e^{s_1 t_n} + B_v e^{s_2 t_n} \tag{2.30}$$

$$i_{Ln} = A_i e^{s_1 t_n} + B_i e^{s_2 t_n} \tag{2.31}$$

Where

$$s_1 = -\frac{1}{2R_n} + \sqrt{\frac{1}{4R_n^2} - 1}$$
$$s_2 = -\frac{1}{2R_n} - \sqrt{\frac{1}{4R_n^2} - 1}$$

- *For* $R_n = 1/2$

$$v_{Cn} = (A_v + B_v t)e^{-t_n} \tag{2.32}$$

$$i_{Ln} = (A_i + B_i t)e^{-t_n} \tag{2.33}$$

- *For* $R_n > 1/2$

$$v_{Cn} = e^{\sigma t_n}(A_v cos(\omega t_n) + B_v sin(\omega t_n)) \tag{2.34}$$

$$i_{Ln} = e^{\sigma t_n}(A_i cos(\omega t_n) + B_i sin(\omega t_n)) \tag{2.35}$$

Where

$$\sigma = -\frac{1}{2R_n}$$
$$\omega = \sqrt{1 - \frac{1}{4R_n^2}}$$

Stage–3 (S_{OFF} **and** D_{OFF})

$$v_{Cn} = v^0_{Cn} e^{-\frac{t_n}{R_n}} \tag{2.36}$$

$$i_{Ln} = 0 \tag{2.37}$$

Thus a converter system in time domain corresponds to a pair of simultaneous equations. Hence the study of converter system in time domain would result in a combined analysis of these equations.

2.4.1 Simulation of Converter Operation in Time Domain

Transient Analysis

The converter equations 2.28 to 2.37 can be solved for any initial condition. The repetitive treatment of these equations would result in the transient response of the converter system. However, it should be noted that, the knowledge of the implimented switching strategy is required to carry out such study.

The algorithm given in figure 2.3 can be applied for a converter operating with constant frequency (f) and constant duty ratio (D). The results obtained by applying this algorithm for a converter having $R_n = 0.7$, D = 0.3 & f = 1 p. u, are shown in figure 2.4. The initial state of the converter is taken as (0,0). The transients in inductor current and capacitor voltage are shown in figure 2.4A and 2.4B, respectively.

Steady State Analysis

It can be observed from figure 2.4 that the given algorithm can be used to determine the steady state operation cycle associated with a given value of on time and off time interval. However, the analytical expression for the capacitor voltage and inductor current, corresponding to the starting point of a steady state cycle, can be obtained from equations 2.28 to 2.37 as shown below.

Consider a steady state operation as shown in figure 2.5, where the states of the converter at the start of *switch off interval* and *switch on interval* are indicated by points 'A' and 'B', respectively. These states can be defined as the *corner states* of the steady state operation cycle.

Thus

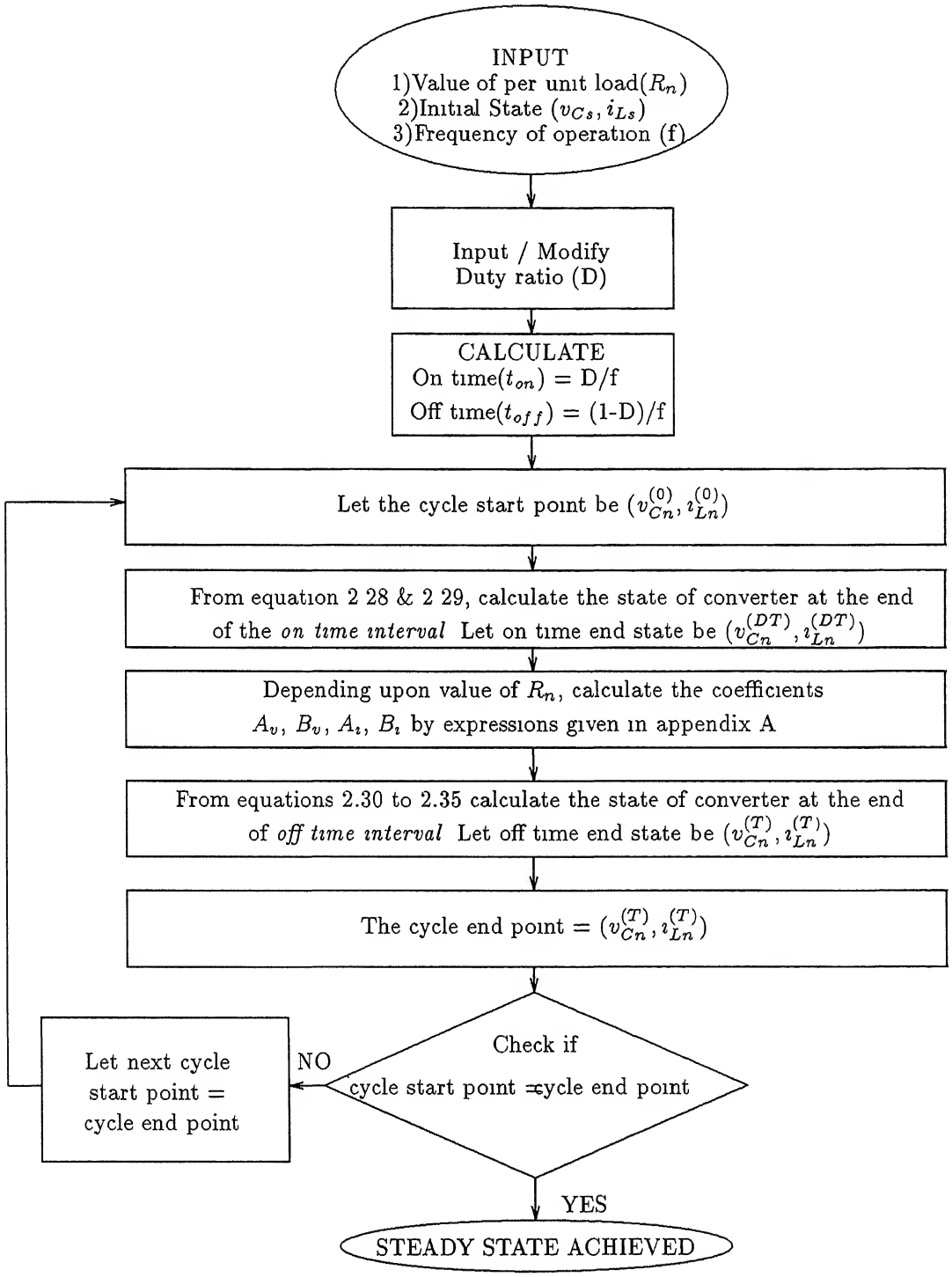

Figure 2.3: Algorithm for simulation of transient operation of converter

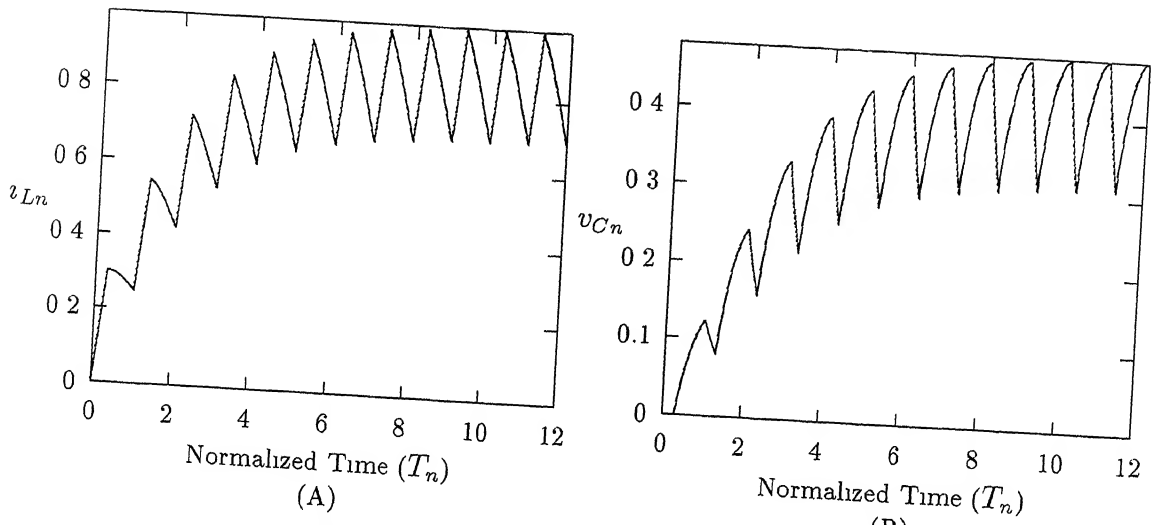

Figure 2.4: A simulation of converter operation

State A can be represented as $\left(v_{Cn}^{(DT)}, i_{Ln}^{(DT)}\right)$.

& State B can be represented as $\left(v_{Cn}^{(T)}, i_{Ln}^{(T)}\right)$.

Let the state of the converter at the start of steady state cycle be $\left(v_{Cn}^{(0)}, i_{Ln}^{(0)}\right)$.

•*For* $R_n < 1/2$

The end state of *off time interval* can be given from equations 2.30 & 2.31 as

$$\begin{bmatrix} v_{Cn}^{(T)} \\ i_{Ln}^{(T)} \end{bmatrix} = \begin{bmatrix} A_v & B_v \\ A_i & B_i \end{bmatrix} \cdot \begin{bmatrix} e^{S_1(1-D)T_n} \\ e^{S_2(1-D)T_n} \end{bmatrix} \tag{2.38}$$

Where A_v, B_v, A_i, & B_i are the constants corresponding to the initial state of switch off interval i. e. $\left(v_{Cn}^{(DT)}, i_{Ln}^{(DT)}\right)$.

During Steady State Condition

$$v_{Cn}^{(T)} = v_{Cn}^{(0)}$$

$$\& \quad i_{Ln}^{(T)} = i_{Ln}^{(0)}$$

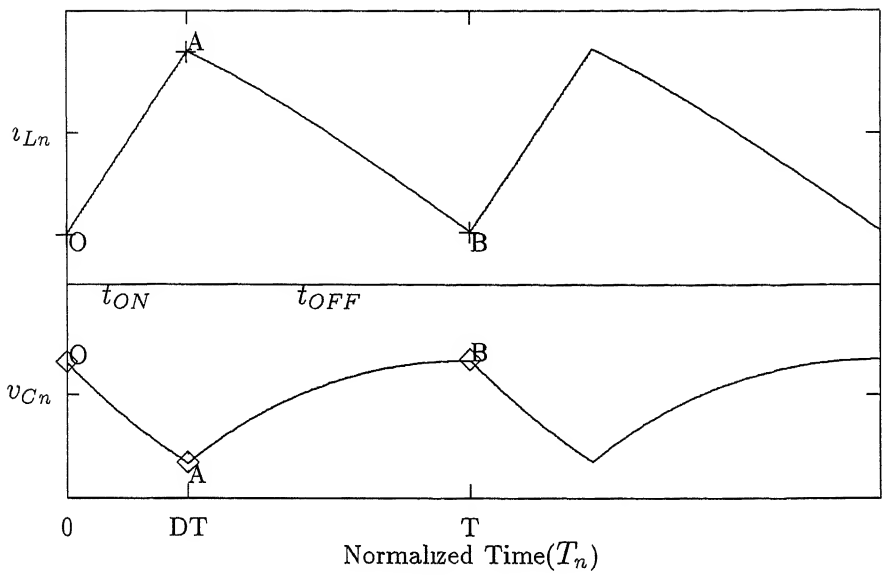

Figure 2.5: A steady state cycle

Hence equation 2.38 can be written as

$$\begin{bmatrix} v_{Cn}^{(0)} \\ i_{Ln}^{(0)} \end{bmatrix} = \begin{bmatrix} A_v & B_v \\ A_i & B_i \end{bmatrix} \cdot \begin{bmatrix} e^{S_1(1-D)T_n} \\ e^{S_2(1-D)T_n} \end{bmatrix} \tag{2.39}$$

From appendix A, the value of A_v, B_v, A_i, & B_i can be substituted in trems of $v_{Cn}^{(DT)}$ & $i_{Ln}^{(DT)}$. Hence the RHS of equation 2.39 can be written as

$$\text{RHS} = \frac{1}{S_1 - S_2} \begin{bmatrix} i_{Ln}^{(DT)} - v_{Cn}^{(DT)} \left(\frac{1}{R_n} + S_2\right) & v_{Cn}^{(DT)} \left(\frac{1}{R_n} + S_1\right) - i_{Ln}^{(DT)} \\ -v_{Cn}^{(DT)} - S_2 i_{Ln}^{(DT)} & v_{Cn}^{(DT)} + S_1 i_{Ln}^{(DT)} \end{bmatrix} \cdot \begin{bmatrix} e^{S_1(1-D)T_n} \\ e^{S_2(1-D)T_n} \end{bmatrix}$$

Substituting for $v_{Cn}^{(DT)}$ & $i_{Ln}^{(DT)}$ from equations 2.28 & 2.29, we get

$$RHS = \frac{1}{S_1 - S_2} \begin{bmatrix} i_{Ln}^{(0)} + DT_n & v_{Cn}^{(0)} e^{-\frac{DT_n}{R_n}} \left(\frac{1}{R_n} + S_1\right) \\ -v_{Cn}^{(0)} e^{-\frac{DT_n}{R_n}} \left(\frac{1}{R_n} + S_2\right) & -i_{Ln}^{(0)} + DT_n \\ -v_{Cn}^{(0)} e^{-\frac{DT_n}{R_n}} & v_{Cn}^{(0)} e^{-\frac{DT_n}{R_n}} \\ -S_2 i_{Ln}^{(0)} - S_2 DT_n & +S_1 i_{Ln}^{(0)} + S_1 DT_n \end{bmatrix} \cdot \begin{bmatrix} e^{S_1(1-D)T_n} \\ e^{S_2(1-D)T_n} \end{bmatrix}$$

$$= \frac{1}{S_1 - S_2} \overbrace{\begin{bmatrix} -\left(\frac{1}{R_n} + S_2\right) e^{S_1(1-D)T_n} e^{-\frac{DT_n}{R_n}} & e^{S_1(1-D)T_n} \\ +\left(\frac{1}{R_n} + S_1\right) e^{S_2(1-D)T_n} e^{-\frac{DT_n}{R_n}} & -e^{S_2(1-D)T_n} \\ -e^{S_1(1-D)T_n} e^{-\frac{DT_n}{R_n}} & S_2 e^{S_1(1-D)T_n} \\ +e^{S_2(1-D)T_n} e^{-\frac{DT_n}{R_n}} & +S_1 e^{S_2(1-D)T_n} \end{bmatrix}}^{P} \cdot \begin{bmatrix} v_{Cn}^{(0)} \\ i_{Ln}^{(0)} \end{bmatrix}$$

$$+ \frac{1}{S_1 - S_2} \underbrace{\begin{bmatrix} DT_n \left(e^{S_1(1-D)T_n} - e^{S_2(1-D)T_n}\right) \\ DT_n \left(S_2 e^{S_1(1-D)T_n} + S_1 e^{S_2(1-D)T_n}\right) \end{bmatrix}}_{Q} \tag{2.40}$$

For a fixed value of R_n, D & T_n, both the matrices of equation 2.40 shown by 'P' and 'Q' are constant matrices. Hence this equation can be written as

$$\begin{bmatrix} v_{Cn}^{(0)} \\ i_{Ln}^{(0)} \end{bmatrix} = c\,[P] \begin{bmatrix} v_{Cn}^{(0)} \\ i_{Ln}^{(0)} \end{bmatrix} + c\,[Q] \tag{2.41}$$

Where

$c = \frac{1}{s_1 - s_2}$

which is a constant for fixed value of R_n

Thus the state of the converter at the start of a steady state cycle can be given as

$$\begin{bmatrix} v_{Cn}^{(0)} \\ i_{Ln}^{(0)} \end{bmatrix} = \left[\frac{1}{c}\,[I] - [P]\right]^{-1} \cdot [Q] \tag{2.42}$$

Where

$[I]$ is a unit matrix.

The similar procedure for other two cases of R_n would give the following results.

• *For* $R_n = 1/2$

$$\left.\begin{aligned} c &= e^{-(1-D)T_n} \\ [P] &= \begin{bmatrix} \left(1+(1-D)(1-\frac{1}{R_n})T_n\right)e^{-\frac{DT_n}{R_n}} & (1-D)T_n \\ (1-D)T_n e^{-\frac{DT_n}{R_n}} & 1+(1-D)T_n \end{bmatrix} \\ [Q] &= \begin{bmatrix} D(1-D)T_n^2 \\ DT_n + D(1-D)T_n^2 \end{bmatrix} \end{aligned}\right\} \quad (2\,43)$$

• *For* $R_n > 1/2$

$$\left.\begin{aligned} c &= e^{(1-D)T_n\sigma} \\ [P] &= \begin{bmatrix} \left(\cos(\theta)+\frac{\sigma}{\omega}\sin(\theta)\right)e^{-\frac{DT_n}{R_n}} & \frac{1}{\omega}\sin(\theta) \\ \frac{-e^{-\frac{DT_n}{R_n}}}{\omega}\sin(\theta) & \cos(\theta)-\frac{\sigma}{\omega}\sin(\theta) \end{bmatrix} \\ [Q] &= \begin{bmatrix} \frac{DT_n}{\omega}\sin(\theta) \\ DT_n\left(\cos(\theta)-\frac{\sigma}{\omega}\sin(\theta)\right) \end{bmatrix} \end{aligned}\right\} \quad (2.44)$$

Where

$$\theta = \omega(1-D)T_n$$

Thus for a given value of R_n, D & T_n, $\left(v_{Cn}^{(0)}, i_{Ln}^{(0)}\right)$ can be calculated by using equation 2.41, subsequently, $\left(v_{Cn}^{(DT)}, i_{Ln}^{(DT)}\right)$ can be calculated by using equations 2.28 & 2.29. Once the two corner points of a steady state cycle are known, we can calculate the average output voltage of the steady state operation cycle by using following equations.

- *For* $R_n < 1/2$

$$V_{Cn_{avg}} = \frac{1}{T_n}\left[R_n\left(v_{Cn}^{(0)} - v_{Cn}^{(DT)}\right) + \frac{1}{s_1 s_2}\left(A_v s_2 e^{(1-D)T_n s_1} + B_v s_1 e^{(1-D)T_n s_2}\right) - \frac{1}{s_1 s_2}\left(A_v s_2 + B_v s_1\right)\right] \quad (2.45)$$

- *For* $R_n = 1/2$

$$V_{Cn_{avg}} = \frac{1}{T_n}\left[R_n\left(v_{Cn}^{(0)} - v_{Cn}^{(DT)}\right) + A_v + B_v\left(1 - e^{(1-D)T}\right) - v_{Cn}^{(0)}\right] \quad (2.46)$$

- *For* $R_n > 1/2$

$$V_{Cn_{avg}} = \frac{1}{T_n}\left[R_n\left(v_{Cn}^{(0)} - v_{Cn}^{(DT)}\right) + \frac{r_1}{r_2}e^{(1-D)T_n\sigma}\sin\left(\omega(1-D)T + \phi - \Delta\right) - \frac{r_1}{r_2}\sin\left(\phi - \Delta\right)\right] \quad (2.47)$$

Where

$$r_1 = \sqrt{A_v^2 + B_v^2}$$
$$\phi = \tan^{-1}\left(\frac{A_v}{B_v}\right)$$
$$r_2 = \sqrt{\sigma^2 + \omega^2}$$
$$\Delta = \tan^{-1}\left(\frac{\sigma}{\omega}\right)$$

2.5 Representation of Converter System in State Space

The equations given in section 2.4 represent v_{Cn} and i_{Ln} as functions of normalized time (t_n). Therefore, a $v_{Cn}(t_n), i_{Ln}(t_n)$ value can be plotted on the state plane of i_{Ln} versus v_{Cn} , with the normalized time (t_n) as an implicit parameter. This results in *State Trajectories* of the system.

The state trajectory which results from state equations during 'ON' period of switch will be referred as *'On time trajectory'*, and the one resulting from state

equations during 'OFF' period of switch will be referred as *'On time trajectory'*. During discontinuos current conduction operation, the 'Off time trajectory' can be divided into two parts corresponding to mode–2 and mode–3.

If the switch 'S' is 'OFF', the system states will follow the Off time trajectory depending upon initial condition of the off time interval. Similarly, if the switch 'S' is 'ON', the system states will follow of the On time trajectory depending upon initial condition of the on time interval. Thus in state space, 'On time' and 'Off time' of the system will be indicated by segments of On time trajectory and Off time trajectory , respectively. Hence the steady state operation of the converter will be portrayed as a closed curve consisting of a single On time trajectory and a single Off time trajectory on state plane. The figure 2.6 shows the *state space representation* of the converter operation studied in section 2.4.1 Two corner points A and B of the steady state cycle (loop) represent the *'Steady state switch off point'* and *'Steady state switch on point'*, respectively.

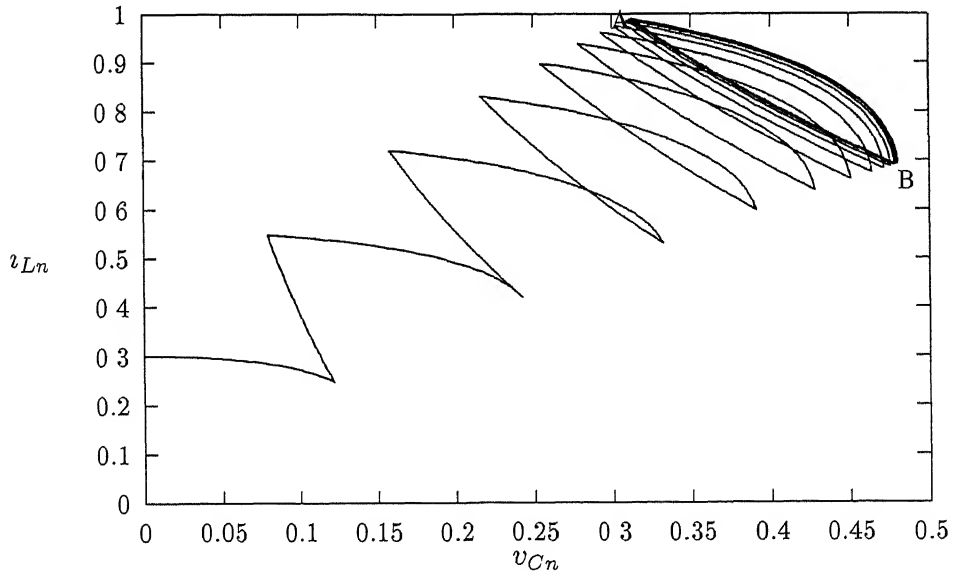

Figure 2.6: A state space representation of converter operation

2.5.1 Derivation of the Equations of The State Trajectories

In order to obtain an explicit relation between state variables v_{Cn} and i_{Ln} , the normalized time can be eliminated from state equations 2.22 to 2.27 as given below. From equations 2.22 & 2.23, by division

$$\frac{di_{Ln}}{dv_{Cn}} = -\frac{R_n}{v_{Cn}} \tag{2.48}$$

Hence the equation of *On time trajectory* is

$$i_{Ln} - i^0_{Ln} = -R_n \ln\left(\frac{v_{Cn}}{v^0_{Cn}}\right) \tag{2.49}$$

Where

C v^0_{Cn} and i^0_{Ln} are initial conditions of v_{Cn} and i_{Ln} respectively

Similarly from equations 2.24 & 2.25, by division

$$\frac{di_{Ln}}{dv_{Cn}} = \frac{R_n v_{Cn}}{v_{Cn} - R_n i_{Ln}} \tag{2.50}$$

This equation can be solved by using substitution of variables, as shown in appendix B. The solution by this method is obtained in the form

$v_{C_n} = f(x)$

Where

$x = \frac{i_{Ln}}{v_{Cn}}$

Which is the slope of the polar vector describing the trajectory.

The constant of integration has been chosen such that $v_{Cn} = V_{C_{peak}}$ at $x = 1/R_n$

The equation of *off time trajectory* thus obtained also has three forms depending upon the value of per unit load (R_n).

- *For* $R_n < 1/2$

$$\ln\left(\frac{v_{Cn}}{v_{C_{peak}}}\right) = -\frac{1}{2}\ln\left(x^2 - \frac{x}{R_n} + 1\right) + \frac{1}{4R_nA}\ln\left(\frac{(2R_nx - 1 - 2R_nA)(1 + 2R_nA)}{(2R_nx - 1 + 2R_nA)(1 - 2R_nA)}\right)$$
$$\ldots\ldots \tag{2.51}$$

Where

$$x = \frac{i_{Ln}}{v_{Cn}}$$
$$\& \; A = \sqrt{\frac{1}{4R_n^2} - 1}$$

- *For* $R_n = 1/2$

$$\ln\left(\frac{v_{Cn}}{v_{C_{peak}}}\right) = -\ln(x-1) + \frac{1}{x-1} - 1 \tag{2.52}$$

- *For* $R_n > 1/2$

$$\ln\left(\frac{v_{Cn}}{v_{C_{peak}}}\right) = -\frac{1}{2}\ln\left(x^2 - \frac{x}{R_n} + 1\right) + \frac{1}{2R_nA}\left[\tan^{-1}\left(\frac{2R_nx-1}{2R_nA}\right) - \tan^{-1}\left(\frac{1}{2R_nA}\right)\right] \tag{2.53}$$

.....

Where

$$x = \frac{i_{Ln}}{v_{Cn}}$$
$$\& \; A = \sqrt{1 - \frac{1}{4R_n^2}}$$

2.6 Features of State Trajectories

The steady state operation of the 'Buck-Boost' converter represented in figure 2.1 is confined to the first quadrant of state plane. Hence the nature of state trajectories has been studied in this quadrant only.

The typical family of 'On time trajectories ' and 'Off time trajectories' for the converter are presented in figure 2.7, where off time trajectories are shown with solid lines and on time trajectories are shown with broken lines. As normalized time is implicit parameter in these trajectories , the arrow head indicates the direction in which system state moves with increasing time. Each trajectory corresponds to a different pair of initial condition (initial state of the system during on time/off time interval). To cover the entire first quadrant of state plane, the initial conditions of

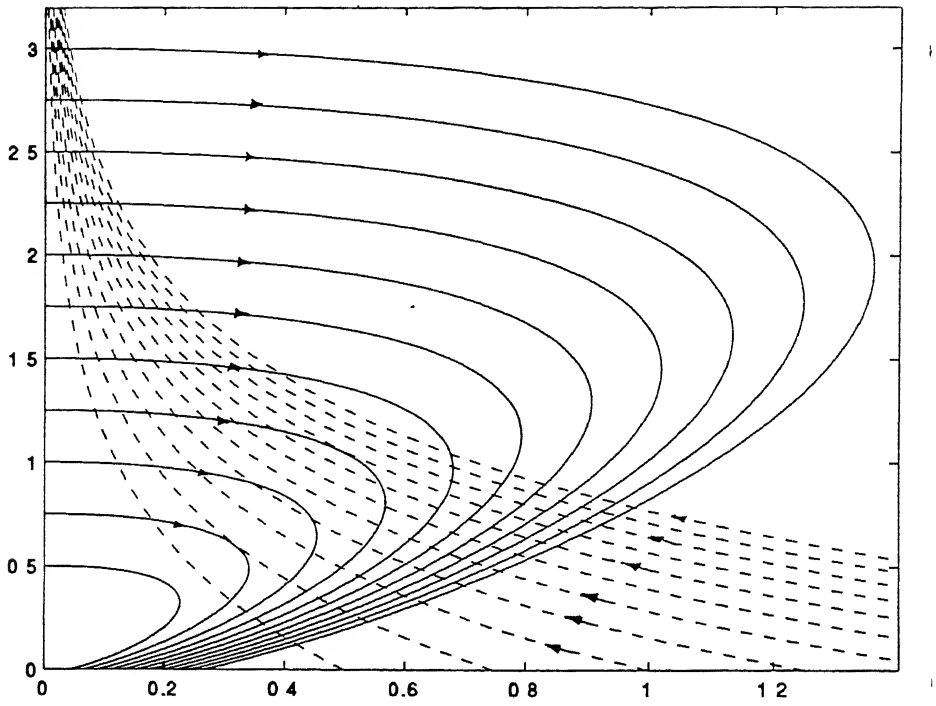

Figure 2.7: A family of *on time trajectory* and *off time trajectory*

On time trajectory are chosen along v_{Cn} axis, and those of Off time trajectory are chosen along i_{Ln} axis.

It can be seen that, the shape and location of both On time trajectory and Off time trajectory depends upon values of R_n and initial state. The study of the variation in state trajectories with variation in R_n and initial condition reveals some important features of converter system.

2.6.1 Variation of State Trajectories with Variation in Initial Condition

For a fixed value of R_n, the location of the state trajectories depend upon the initial condition of the system during respective intervals. The study of the variation in state trajectories with variation in initial condition is useful to obtain the family of state trajectory.

Variation in On Time Trajectory

Let the initial condition of an *on time trajectory* along v_{Cn} axis be $(V_{Cn}(0), 0)$, where $V_{Cn}(0)$ denotes the value of $(v^0_{Cn})_{on}$ along the v_{Cn} axis. The equation of on time trajectory (i. e. equation 2.49) can then be written as

$$i_{Ln} = -R_n \ln\left(\frac{v_{Cn}}{V_{Cn}(0)}\right) \tag{2.54}$$

Hence all the points which have same $\frac{v_{Cn}}{V_{Cn}(0)}$ ratio have same value of i_{Ln}. Therefore one reference curve can be made for $V_{Cn}(0) = 1$. The other curves can be derived from this reference curve by multiplying v_{Cn} and $V_{Cn}(0)$ by same scaling factor.

Variation in Off Time Trajectory

The *off time trajectory* can be obtained by using equations 2.51 to 2.53. However, these equations do not explicitly include the initial condition of the off time interval and require the knowledge of $v_{C_{peak}}$. Hence as explained in section 2.5, the equations 2.30 to 2.35 can be used to obtain the off time trajectory from the knowledge of initial condition. The constants A_v, B_v, A_i, B_i are calculated by the expressions given in appendix A.

Let the initial condition of an *off time trajectory* along i_{Ln} axis be $(0, I_{Ln}(0))$, where $I_{Ln}(0)$ denotes the value of $(i^0_{Ln})_{off}$ along the i_{Ln} axis. The constants A_v, B_v, A_i, B_i can then be expressed as given below.

	$R_n < 1/2$	$R_n = 1/2$	$R_n > 1/2$
A_v	$\frac{I_{Ln}(0)}{s_1 - s_2}$	0	0
B_v	$-\frac{I_{Ln}(0)}{s_1 - s_2}$	$I_{Ln}(0)$	$\frac{I_{Ln}(0)}{\omega}$
A_i	$-\frac{I_{Ln}(0)s_2}{s_1 - s_2}$	$I_{Ln}(0)$	$I_{Ln}(0)$
B_i	$\frac{I_{Ln}(0)s_1}{s_1 - s_2}$	$I_{Ln}(0)$	$-\frac{I_{Ln}(0)\sigma}{\omega}$

B

It can be seen from the above expressions of the constants and equations 2.30 to 2.35 that, if $I_{Ln}(0)$ is changed by a scale factor, say λ , then for same value of time(t_n),

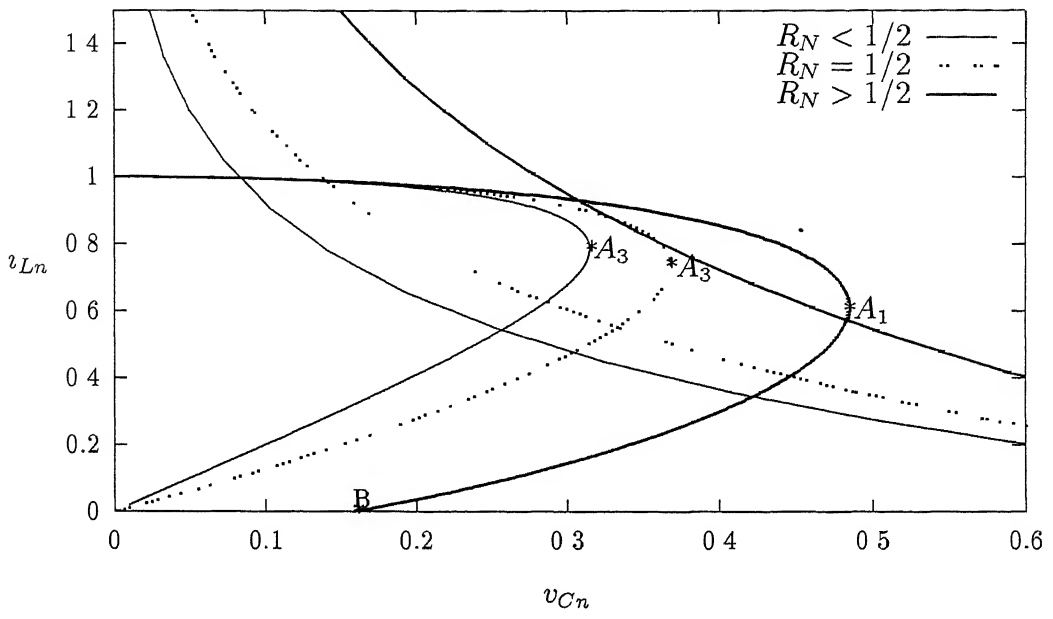

Figure 2 8: The variation of trajectories with R_n

v_{Cn} & i_{Ln} also change by the same scale factor. Thus, if we calculate the off time trajectory for $I_{Ln}(0) = 1$, the other trajectories can be calculated by scaling.

Hence the *on time trajectory* for $V_{Cn}(0) = 1$ and, the *off time trajectory* for $I_{Ln}(0) = 1$ can be refered as *reference trajectories.*

2.6.2 Variation of State Trajectories with Variation in Per Unit Load

The shape of both On time trajectory and Off time trajectory depends upon values of R_n. Figure 2.8 shows on time trajectories and off time trajectories for various values of R_n and fix value of initial state.

It can be observed that the general nature of On time trajectory does not change with variation in per unit load (R_n). However the nature of Off time trajectory can be broadly classified as

- *For* $Rn \leq 1/2$

  The Off time trajectory moves towards origin of state plane with increasing time, and reaches origin as $t_n \rightarrow \infty$.

- *For* $R_n > 1/2$

  The Off time trajectory will have a non zero intersection with v_{Cn} axis(as shown by point B in figure 2.8). This point will have a finite time corresponding to it. If system *Off time period* is more than this time, further Off time trajectory will move towards origin, along v_{Cn} axis.

The portion of *Off time trajectory* along v_{Cn} axis corresponds to the mode–3 (figure 2.2C), which indicates a discontinuous mode of operation. The non zero intersection point B in figure 2.8 represents the boundary between continuos and discontinuous modes, and hence will be referred as *boundary point.* Thus it can be concluded that, a converter system can have discontinuous mode of operation only if per unit load is more than 1/2 and the system Off period exceeds the time corresponding to boundary point time. Hence the knowledge of boundary point will be helpful to decide the mode of operation. The following expression, derived from equation 2.35 by eqating i_{Ln} to zero, gives boundary point time as

$$t_{n_{boundary}} = \frac{1}{\omega}\left[\pi + \tan^{-1}\left(-\frac{A_i}{B_i}\right)\right] \tag{2.55}$$

2.6.3 Uniqueness of a Steady State Operation

For a fix value of R_n, there exists a *one and only one* pair of *on time trajectory* and *off time trajectory* passing through any point in state space (i. e. state of converter), specified as a corner point of a steady state operation. Hence there will be a unique steady state associated with any point in state space.

2.6.4 Peak Voltage Point of Off Time Trajectory

The study of equation 2.50 shows that for a fixed value of R_n, Off time trajectories can be subdivided into three parts such as

- Negative slope region when $v_{Cn} < R_n i_{Ln}$
- Positive slope region when $v_{Cn} > R_n i_{Ln}$
- Infinite slope point when $v_{Cn} = R_n i_{Ln}$

This also indicates that the Off time trajectory will have peak normalized capacitor voltage when the following relationship is satisfied

$$v_{Cn} = R_n i_{Ln} \tag{2.56}$$

The point in the state space corresponding to these values of v_{Cn} and i_{Ln} can be called as *peak voltage points* (as shown by point 'A_1','A_2','A_3' in figure 2.8). From equations 2.30 to 2.35 & 2.56. time corresponding to peak voltage point can be derived as

- *For* $R_n < 1/2$

$$t_{n_{peak}} = \frac{1}{s_2 - s_1} \ln\left(\frac{A_v - R_n A_i}{R_n B_i - B_v}\right) \tag{2.57}$$

- *For* $R_n = 1/2$

$$t_{n_{peak}} = \left(\frac{A_v - R_n A_i}{R_n B_i - B_v}\right) \tag{2.58}$$

- *For* $R_n > 1/2$

$$t_{n_{peak}} = \frac{1}{\omega} \tan^{-1}\left(\frac{A_v - R_n A_i}{R_n B_i - B_v}\right) \tag{2.59}$$

2.6.5 Tangent Point of the Off Time Trajectory

As explained in section 2.5, the closed curve obtained by intersection of on time trajectory and off time trajectory represents a steady state operation of the converter system. The figure 2.9 shows a single off time trajectory, selected arbitrarily. The various steady state operations associated with this off time trajectory are A_1TB_1, A_2TB_2 etc. It can be seen from this figure that, at point T, both the on time trajectory and off time trajectory are tangential to each other. Hence, this point can be referred as a *tangent* point. Any on time trajectory, to the right of the trajectory, O'TY will not have an intersection with the off time trajectory OTX . It can also be seen from the figure 2.9 that, all steady state operations associated with off time trajectory (OTX) will have the two corner points on the two sides of point T. Thus the tangent point T can be considered to divide the off time trajectory OTX in two portions such that

Portion OT → Which includes the *steady state switch off points* of all steady state operations associated with OTX

Portion TX → Which includes the *steady state switch on points* of all steady state operations associated with OTX

Hence, it can be concluded that all steady state operations associated with any off time trajectory must include the tanjent point T of that off time trajectory.

Physical Significance of the Tangent Point

It can be seen from figure 2.9 that, as the on time trajectory moves closer to the trajectory O'TY from left, the resulting close curve (steady state operation) contracts about point T. Also the frequency of resulting steady state operation increases, and average state of the steady state cycle approaches the tangent point T.

In the limiting case, that is for converter having a steady state operation at tangent point, on time and off time intervals will be zero. Hence, the frequency of

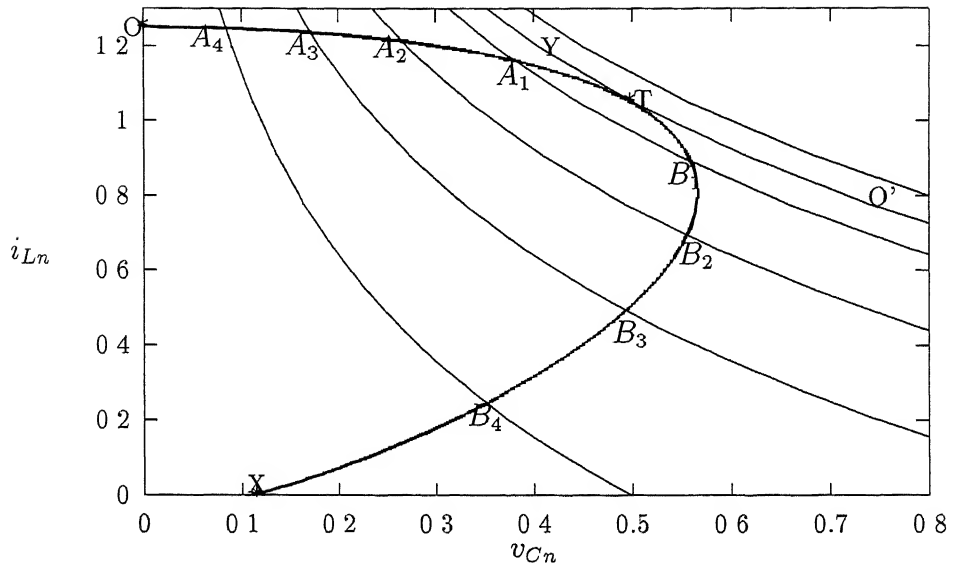

Figure 2.9: The concept of a tangent point of off time trajectory

operation will be infinite. During such operation the capacitor voltage and inductor current will be constant throught the operation and hence the average state of steady state cycle will be a tangent point itself.

Thus it can be said that a tangent point represents an ideal operation of converter at the high frequency.

The detailed simulation of various steady state operation in vicinity of tangent point (as carried out in chapter 3 and shown with the help of performance curves) gives the following results.

- The average state of the steady state cycle, for converter operating in low ripple region (below 5%) can be approximated as the tangent point.

- For the steady state operation, in vicinity of the tangent point, inductor current and capacitor voltage can be assumed to be varying linearly with time. Hence the converter analysis can be carried out as shown in appendix D. The

various parameter/variables of the converter can be expressed as given below

$$V_{Cn_{av}} = V_{op_{av}} \approx \frac{D}{1-D} \quad (\text{since } V_{in} = 1p.u) \tag{2.60}$$

$$I_{Ln_{av}} = I_{O_{av}} \frac{1}{1-D} = \frac{V_{op_{av}}}{R_n} \frac{1}{1-D} \tag{2.61}$$

Mathematical Representation of a Tangent Point

From equation 2.50, the slope of off time trajectory is given as

$$\rho_{off} = \frac{di_{Ln}}{dv_{Cn}} = \frac{R_n v_{Cn}}{v_{Cn} - R_n i_{Ln}} \tag{2.62}$$

Similarly from equation 2.48, the slope of the on time trajectory is given as

$$\rho_{on} = \frac{di_{Ln}}{dv_{Cn}} = -\frac{R_n}{v_{Cn}} \tag{2.63}$$

At tangent point

$$\rho_{off} = \rho_{on} \tag{2.64}$$

Hence from equations 2.62, 2.63 & 2.64, we get

$$v_{Cn}(1 + v_{Cn}) = R_n i_{Ln} \tag{2.65}$$

Thus the point in the state space which satisfies the equation 2.65 will be a tangent point of the off time trajectory

2.6.6 Output Energy in a Steady State Cycle

The Off time trajectory can also reveal the total energy given to the load. This can be seen as follows.

By rearranging equation 2.50, we get

$$(v_{Cn} - R_n i_{Ln}) di_{Ln} = R_n v_{Cn} dv_{Cn} \tag{2.66}$$

Let us consider a steady state cycle as shown in figure 2.10.

By integrating equation 2.66 from point A to B, we get

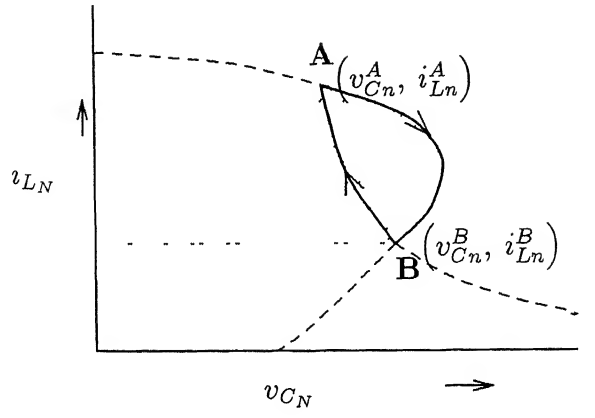

Figure 2.10: The output energy in a steady state operation

$$\begin{aligned}\int_{i_{Ln}^A}^{i_{Ln}^B} v_{Cn} di_{Ln} &= R_n \left[\int_{i_{Ln}^A}^{i_{Ln}^B} i_{Ln} di_{Ln} + \int_{v_{Cn}^A}^{v_{Cn}^B} v_{Cn} dv_{Cn} \right] \\ &= \frac{R_n}{2} \left[\left(i_{Ln}^{B^2} + v_{Cn}^{B^2} \right) - \left(i_{Ln}^{A^2} + v_{Cn}^{A^2} \right) \right] \end{aligned} \quad (2\ 67)$$

As shown in appendix C, the quantity $(i_{Ln}^2 + v_{Cn}^2)$ is a normalized stored energy. Hence equation 2.67 can be written as

$$\begin{bmatrix} \text{Area between the off time} \\ \text{trajectory and } i_{Ln} \text{ axis} \end{bmatrix} = \frac{R_n}{2} \begin{bmatrix} \text{Change in normalized stored} \\ \text{energy} \end{bmatrix} \quad (2\ 68)$$

However, it can be seen from figure 2.2B that there is no input source during Off period of the switch. Hence change in stored energy must be equal to energy given to the load. Thus, the output energy can be calculated from the knowledge of steady state loop on state space.

2.7 Conclusion

The idealized Buck–Boost converter has been studied in the time domain and state space. The analytic equations of the system state trajectories has been developed, where the equation of the off time trajectory is expressed in terms of the slope $(\frac{i_{Ln}}{v_{Cn}})$ of the polar vector describing the trajectory. The various features of the state trajectories have been studied, and the information of the converter system revealed

by these features has been brought out. Further a method has been proposed for scaling the state plane trajectories for obtaining family of the state trajectory. The approximate model neglecting the ripple has been related to the state space trajectories by defining a *Tangent point.* Finally the energy given to the load has been shown to be equal to the area under the off time trajectory and i_{Ln} axis.

Chapter 3

The Design Curves Based On State Space Analysis

The analysis given in chapter 2 has been used to obtain the design curves for the Buck–Boost converter. The section 3.1 highlights the need of performance curves of a converter. The section 3.2 explains the detailed procedure involved in calculating the performance curves. The curves of T_{on} vs T_{off}, D vs T_n, $V_{O_{av}}$ vs T_n & %ripple vs T_n have been calculated and plotted for a wide range of the converter operations. A design example based on these performance curves is given in section 3.3.

3.1 Performance Curves of the Converter

It has been shown in section 2.4.1 that, for a fixed operating condition i. e. for a given values of *per unit load(R_n), duty ratio(D) and operating frequency(f)*, the steady state operation of the converter can take place between a unique pair of corner states. These corner states can be calculated from equations 2.42 to 2.44. The output characteristics of the converter i. e. the average output voltage(r_{v_0}) & the ripple in output voltage($V_{O_{rip}}$) can be calculated from equations 2.45 to 2.47.

However, for a designer of the converter system, as well as for the a designer of the controller, it is essential to find out the unique operating condition for a

desired output characteristic. Due to the nature of the system equations, it is not possible to analytically determine the operating condition from the knowledge of the desired output characteristic. Hence for this purpose, the output characteristics can be calculated for various operating conditions . The performance curves can be obtained by plotting the output characteristic versus the operating condition. The state space representation of the converter can be effectively used for this purpose.

3.2 State Space Analysis of Converter

As explained in section 2.5 (figure 2.6), any closed curve on state space comprising of single *on time trajectory* and a single *off time trajectory* represents a steady state operation of the converter. Hence the study of various intersections of off time trajectories and on time trajectories will result in the study of various operating conditions.

3.2.1 Algorithm for State Space Analysis

To study the various intersections of the two families of trajectory, the algorithm given in figure 3.1 can be used, where the initial condition of the of the off time interval, along the i_{Ln} axis(i. e. $I_{Ln}(0)$) and per unit load resistance(R_n) are systematically varied over the range $\left(I_{Ln_0}(0) \ldots I_{Ln_p}(0) \ldots I_{Ln_{limit}}(0)\right)$ & $\left(R_{n_0} \ldots R_{n_j} \ldots R_{n_{limit}}\right)$, respectively. The *off time trajectory* for each value of $I_{Ln_p}(0)$ is calculated by scaling (i. e. multiplying by $I_{Ln_p}(0)$) the *reference off time trajectory* as explained in section 2.6.1. It should be noted that the time is not being scaled as it is already normalized while calculating the reference off time trajectory.

The various steady state operations associated with a *off time trajectory* can be found out by selecting the various points on any one side of the tangent point as one corner state. The corresponding second corner state can then be calculated by an algorithm given in figure 3.2. For faster computation, this algorithm uses the technique of *Binary Search* till the search range is reduced to consecutive points in

the look up table. Thereafter the finer search is carried out using the exact equations of *off time trajectory* (2 30 to 2.35).

Results of State Space Analysis

The results obtained by applying this algorithm are shown in figures 3.3 to 3.9, where each figure presents a family of *performance curves* for a fixed value of per unit load(R_n). The value of $I_{Ln}(0)$ is varied from 0.25 to 5 *pu* in step of 0.25, and the values of R_n is selected between 0.3 to 3 *pu*.

The comparative study of the various steady state operations over the wide range can be done with the help of these *performance curves.* However,it should be noted that in most of the practical cases, the converter is required to operate in low ripple region. Hence the study of the performance curves in this region enables one to understand the various features of converter operation in this region. The figure 3.9 shows the enlarged portion of figure 3.4 (i.e. for $R_n = 0.9$) for ripple below 5from the study of these curves are as follows.

1. For a fixed value of R_n and a given value of *(D & T_n) or ($V_{O_{avg}}$ & T_n)*, the converter will have the *unique steady state operation.*

2. During the low ripple steady state operation, *duty ratio(D) and the average output voltage($V_{O_{avg}}$)*are approximately constant for a fixed value of $I_{Ln}(0)$, and do not vary with the switching frequency. In such cases the voltage can be determined independently, for a given value of switching frequency.

3. For a fixed value of output voltage ripple, there is a minimum required switching frequency. This value decreases as R_n increases. The maximum switching frequency depends on of the power switch.

4. For a constant operating frequency, the output voltage ripple incerases with incerase in average output voltage.

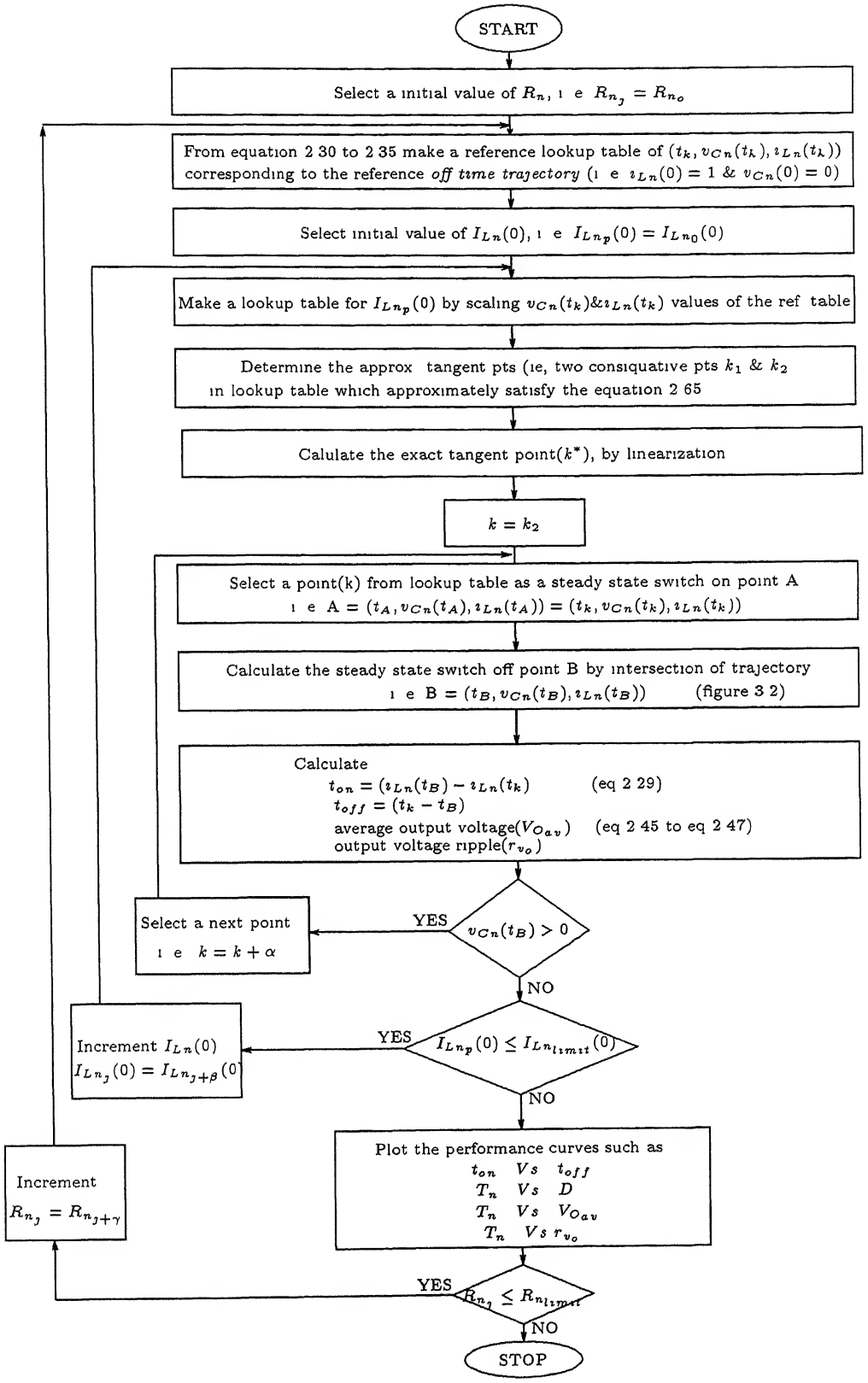

Figure 3.1: Flow chart to study various operating conditions

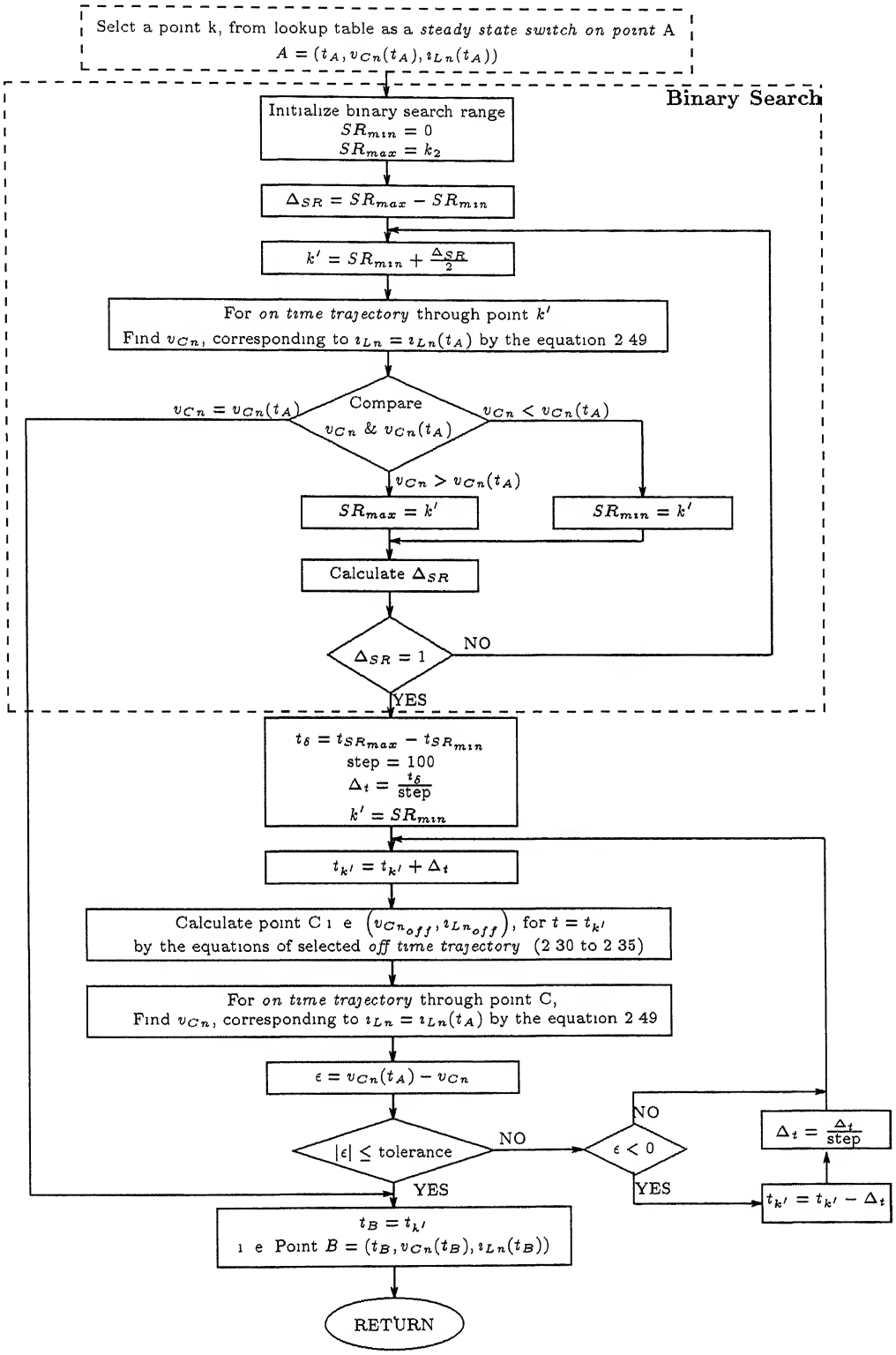

Figure 3.2: Flow chart to find out intersections points

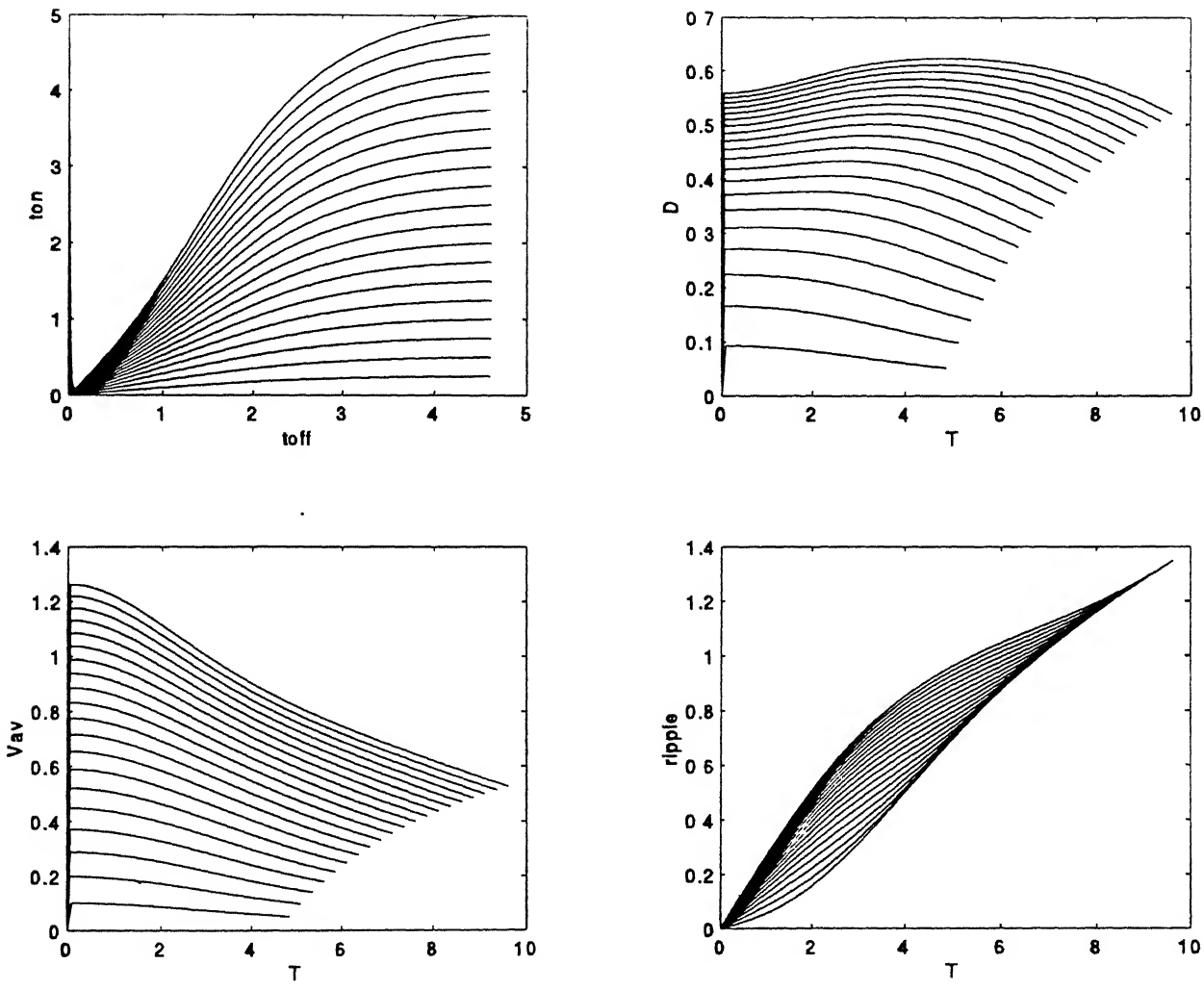

Figure 3.3: The performance curves for $R_n = 0.6$

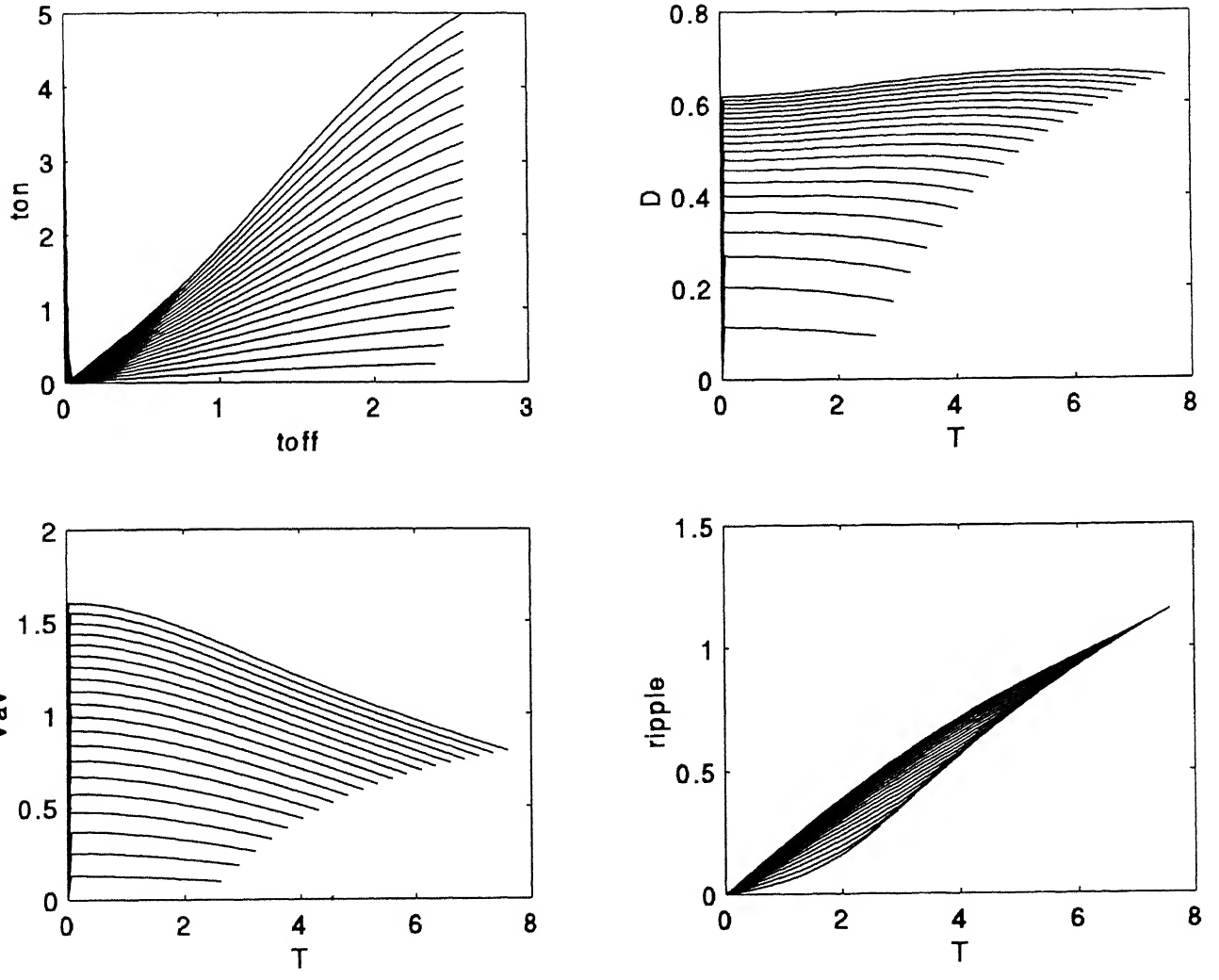

Figure 3.4: The performance curves for $R_n = 0.9$

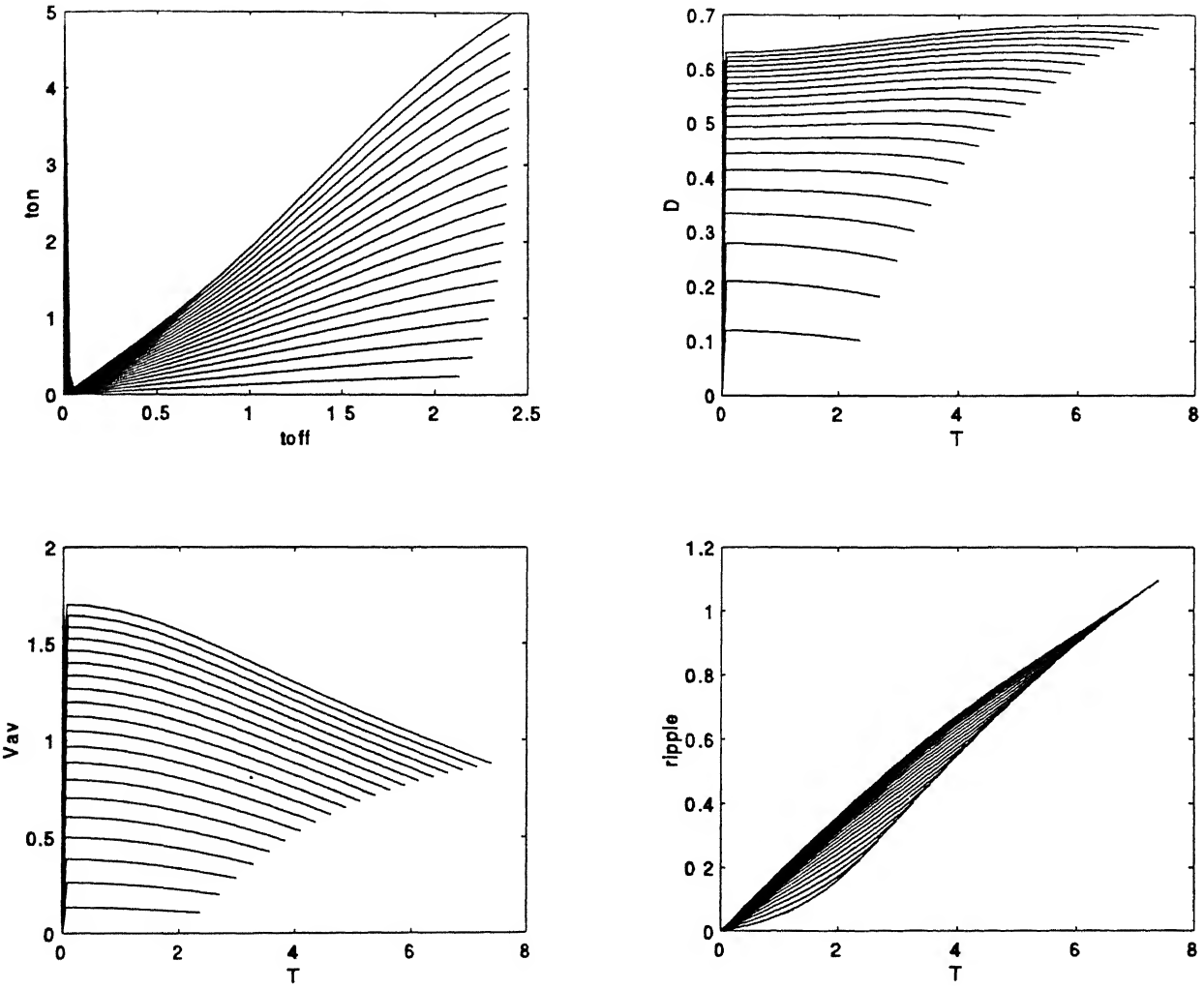

Figure 3.5: The performance curves for $R_n = 1$

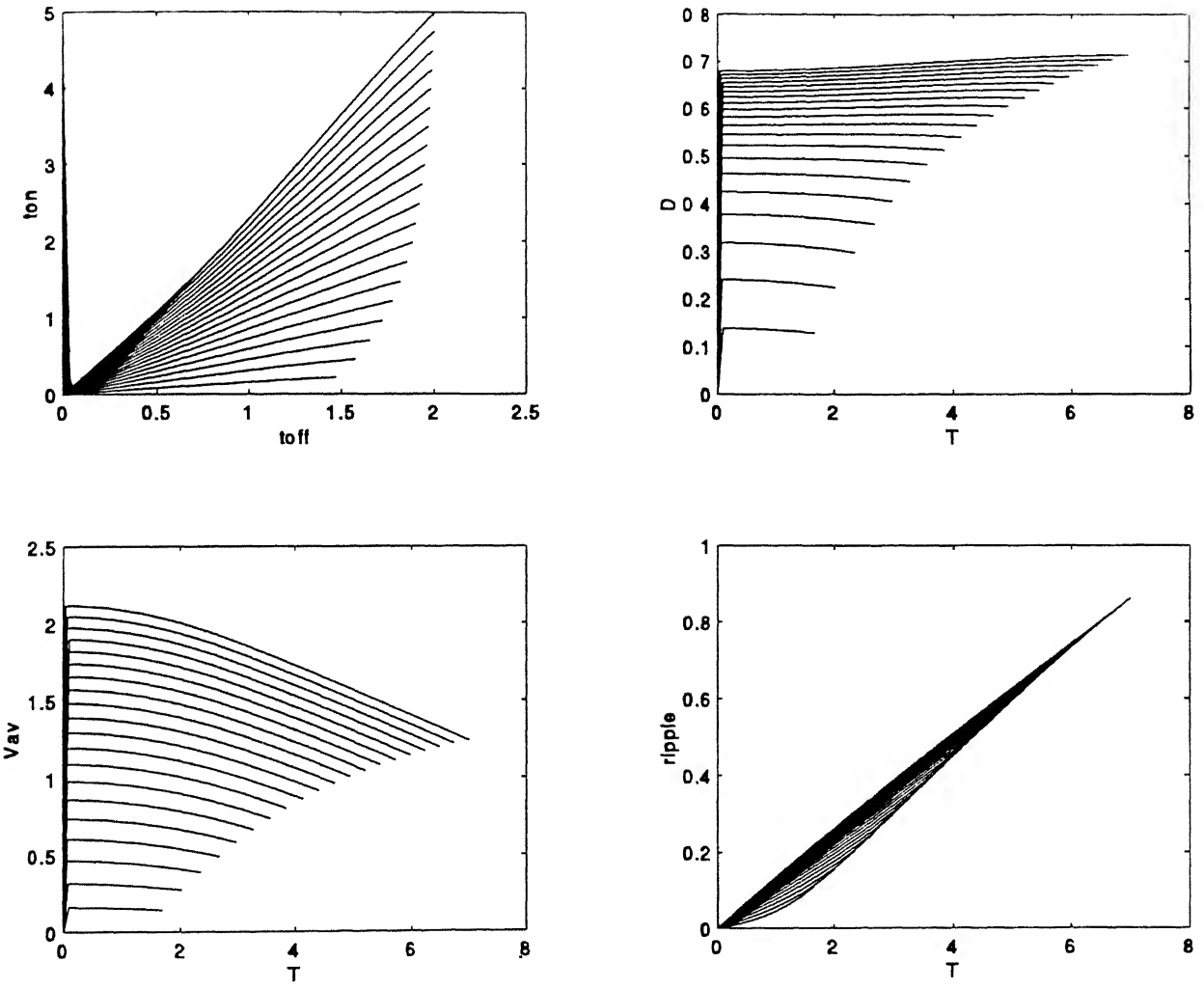

Figure 3.6: The performance curves for $R_n = 1.5$

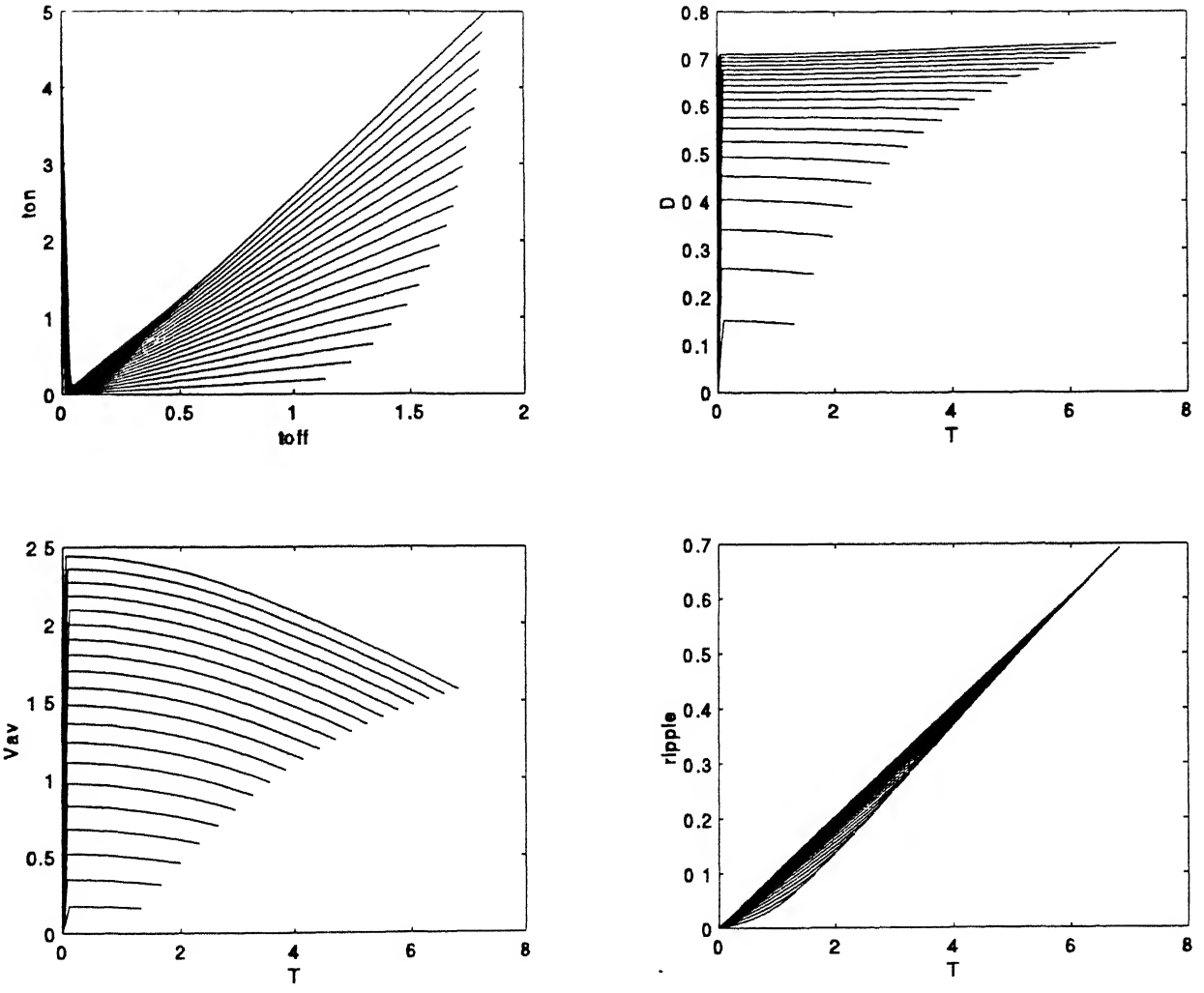

Figure 3.7: The performance curves for $R_n = 2.0$

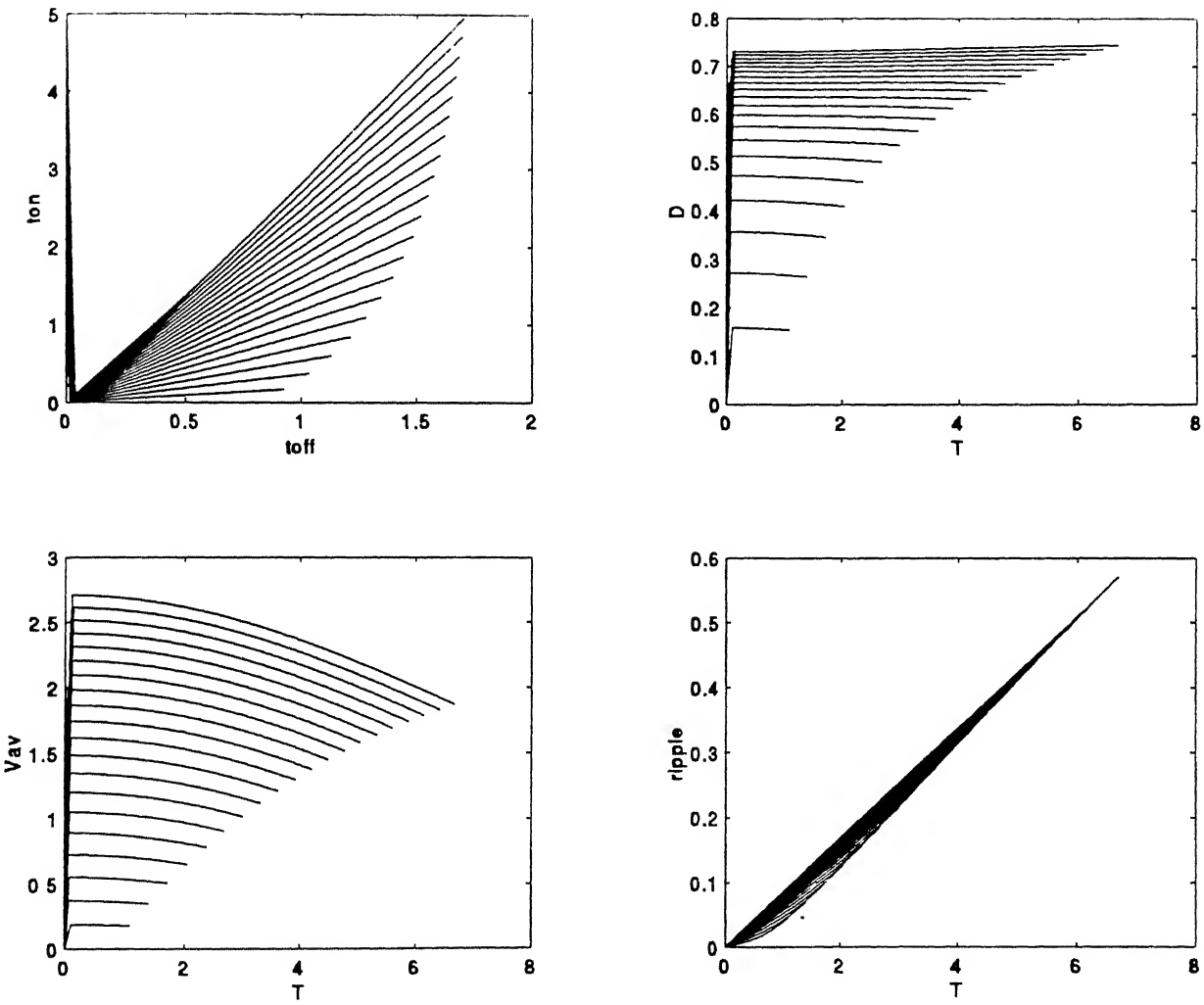

Figure 3.8: The performance curves for $R_n = 2.5$

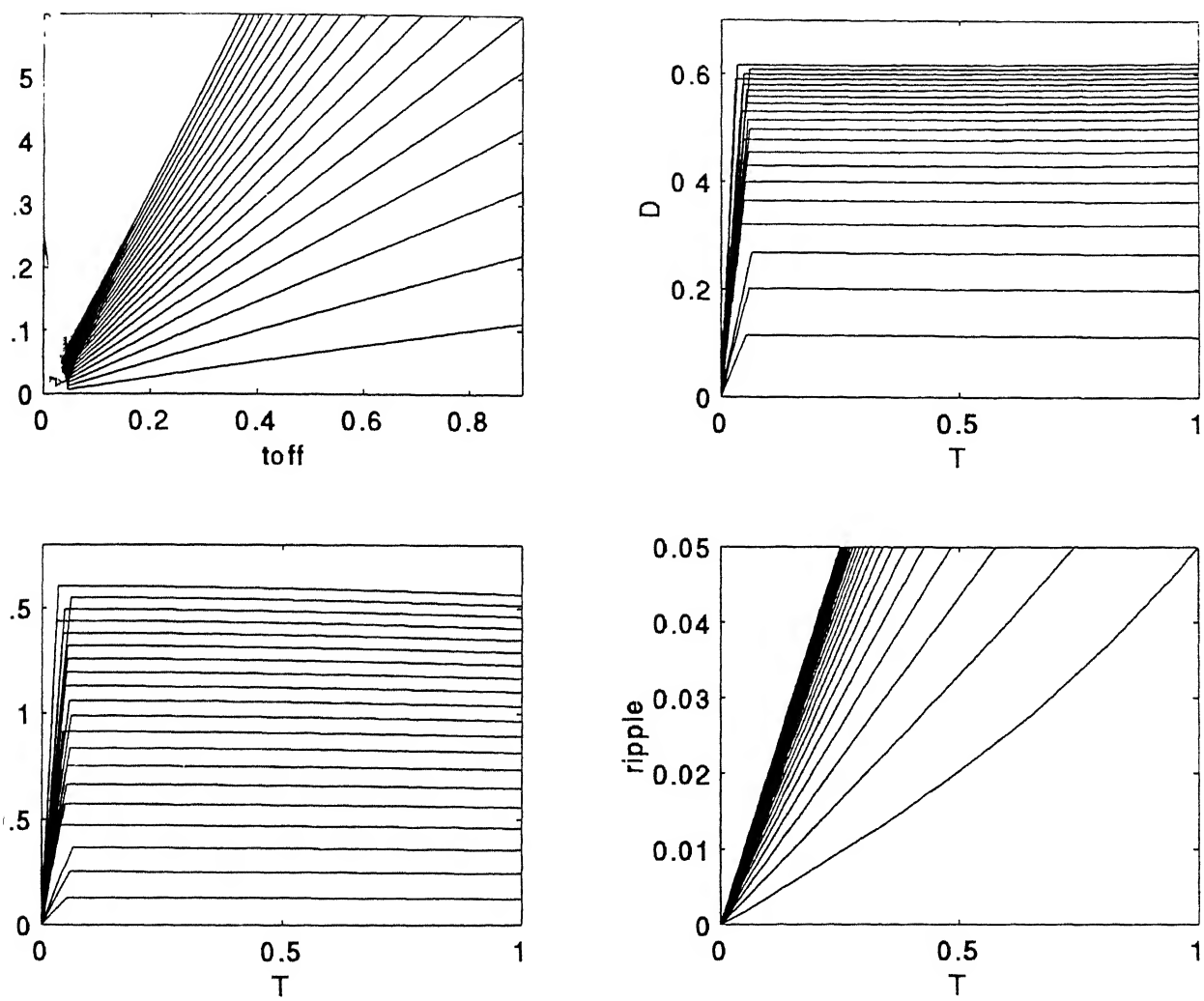

Figure 3.9: The performance curves in the low ripple region for $R_n = 0.9$

3.3 Design of Converter

With the help of these performance curves, it is possible to determine the exact operating conditions required to produce a desired output characteristic of the converter. This feature enables an accurate design of the converter to meet the required characteristic. The procedure of designing a converter is shown in figure 3.10, where value of the required ripple is assumed to be low (i. e. below 10%). It can be seen that, this algotithm gives the various suitable values of inductor and capacitor. The selection of exact values of L and C can be done by a trade off between these two quantities.

The design procedure has been carried out using the above algorithm for a converter having the following data

- Input voltage(V_{in}) = 48 V
- Average output voltage($V_{O_{av}}$) = 12 V
- Average output current($I_{O_{av}}$) = 1 A
- permissible output voltage ripple = 5%
- permissible operating frequency = 8 KHz

The figure 3.11 shows the variation of L & C values with change in normalized load resistance(R_n), obtained from the above algorithm. However for a given value of output power and output voltage, the value of load resistance in Ω is fixed. Hence the figure 3.11 allows us to see the variation of required L & C values for different assumed values of R_n. It can be seen that as R_n is increased, the value of L is reduced and the value of C is increased. The reduction in value of L is negligible after R_n = 2.5 p. u. Therefore L & C can be chosen corresponding to R_n equal to two. Thus the selected values of inductor and capacitor are 0.42mH and 18.65 μF. The calculation according the flow chart(figure 3.10) also gives the following data :-

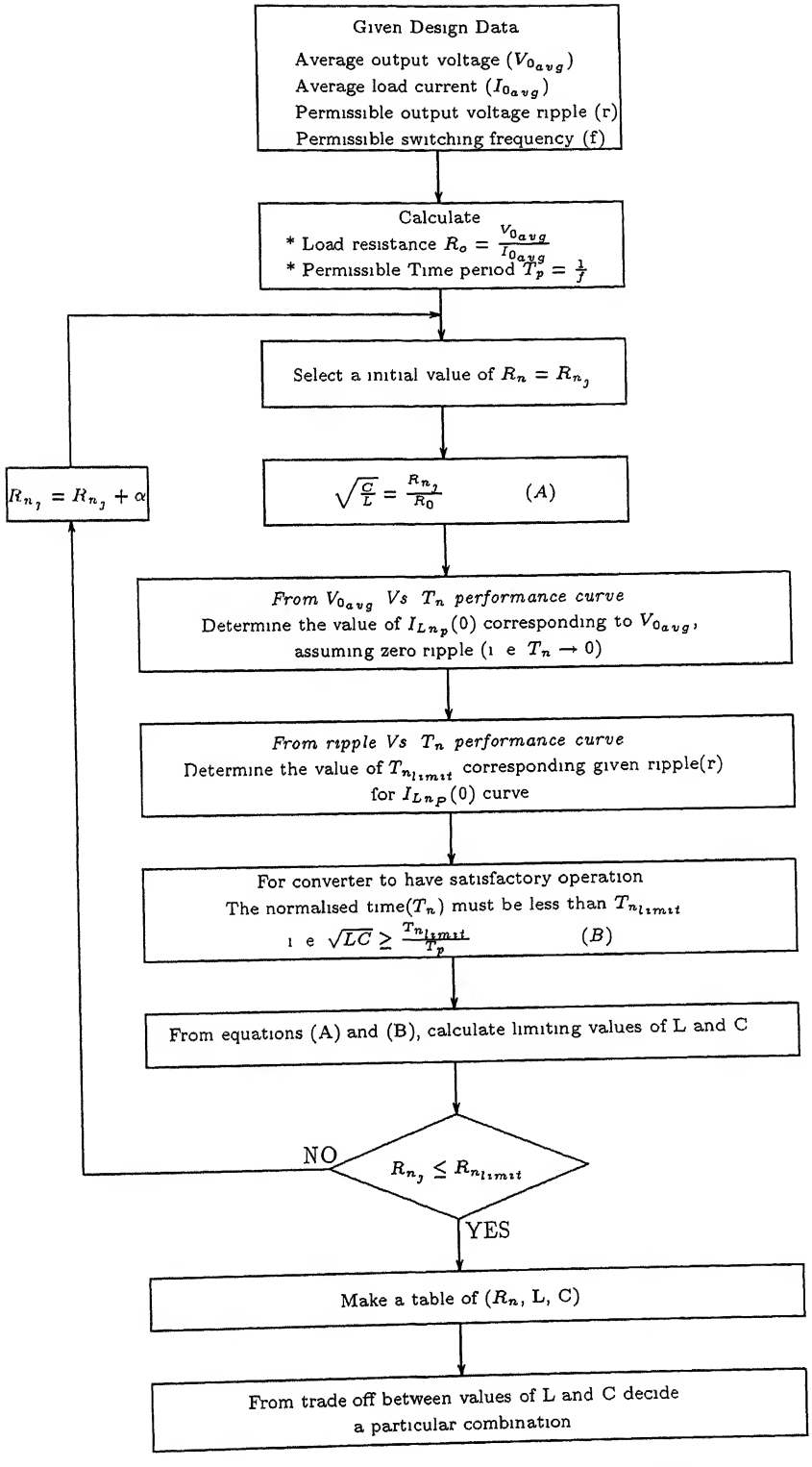

Figure 3.10: Flow chart for design of converter

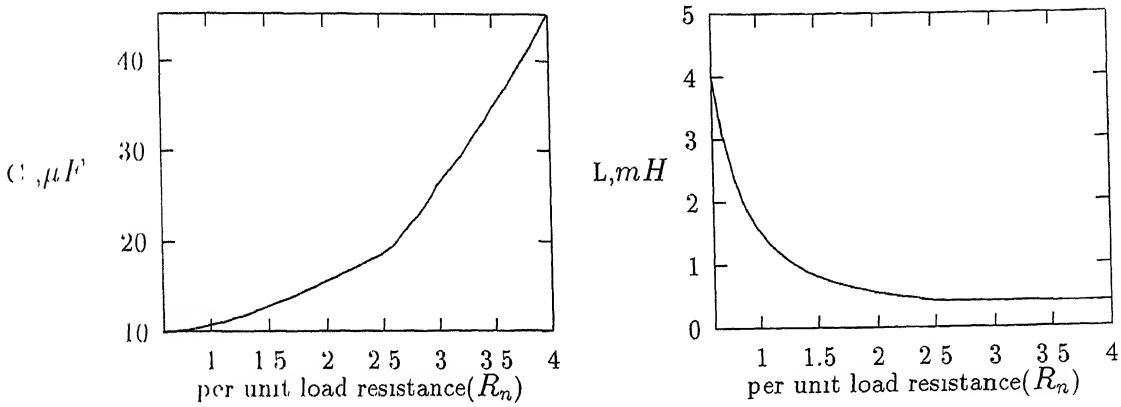

Figure 3.11: Simulation of Converter Operation

$$D = \frac{V_{O_{av}}}{V_{O_{av}} + V_{in}} = 0.2$$

$$I_{L_{av}} = \frac{I_{O_{av}}}{1 - D} = 1.25$$

Hence the semiconductor power switch will carry a pulse of 1.25 A peak with 20% duty cycle, operating at 8KHz. The diode is carrying a pulse of 1.25 A peak with 80% duty cycle . Suitable semiconductor devices can be chosen on the basis of the above data.

3.4 Conclusion

The analysis given in chapter 2 has been used in this chapter to obtain the detailed design curves of the Buck–Boost converter. A design example of a 12 V , 1A converter has been worked out .

Chapter 4

The Study of Various Controllers

The only means available for controlling the rate of flow of electrical energy from source to load in a DC-DC converter, is the switching on and off the power switch. The behavior of the converter system is very much dependent on the manner in which the controller(control system) generates the switching sequence for the power switch. Hence for the effective design of the controller it is necessary to understand the cause and effect relationships which exist between the action of the controller and the resultant converter performance.

The state space analysis technique, discussed in the previous chapters provide a theoretical insight into the fundamental nature of the converter operation. Hence this technique can be used to understand the manner in which the various control techniques accomplish the task of determining a switching sequence of the power switch [1][2]. The conceptual visualization of the controller action, enables one, to postulate various control laws which will improve the system performance.

4.1 Control Using Input current Limit and Output Voltage Limit (I_{in}&V_{out} controller)

In a DC DC converter the input current and output voltage can be controlled by controlling the inductor current(i_{Ln}) and capacitor voltage(v_{Cn}) respectively. It can be seen from the nature of the state trajectories that:-

- During on time interval, the inductor current(i_{Ln}) increases and capacitor voltage(v_{Cn}) decreases.
- During off time interval, the capacitor voltage(v_{Cn}) increases upto a particular peak value and decreases thereafter, whereas the inductor current(i_{Ln}) decreases continuously.

Hence the inductor current and capacitor voltage can be controlled by controlling the on time and off time interval respectively. If the limits of these quantities are specified the switching sequence can be generated by the logic diagram given in figure 4.1. It should be noted that the duty ratio(D) and switching frequency(f) are not explicitly controlled in this technique.

4.1.1 Action of the Controller

The function of the controller can be explained with the help of some generalized cases of converter operation. Consider an arbitrary voltage and current limits say $V_{Cn_{lim}}$ and $I_{Ln_{lim}}$ respectively. These limits can be represented by two lines on the state space as shown in figure 4.2, where line XO' represents voltage limit and line YO' represents the current limit. It can be seen from this figure that these two lines divide the state space in four region as given below.

Region–I :- $v_{Cn} < V_{Cn_{lim}}$ and $i_{Ln} < I_{Ln_{lim}}$

Region–II :- $v_{Cn} > V_{Cn_{lim}}$ and $i_{Ln} < I_{Ln_{lim}}$

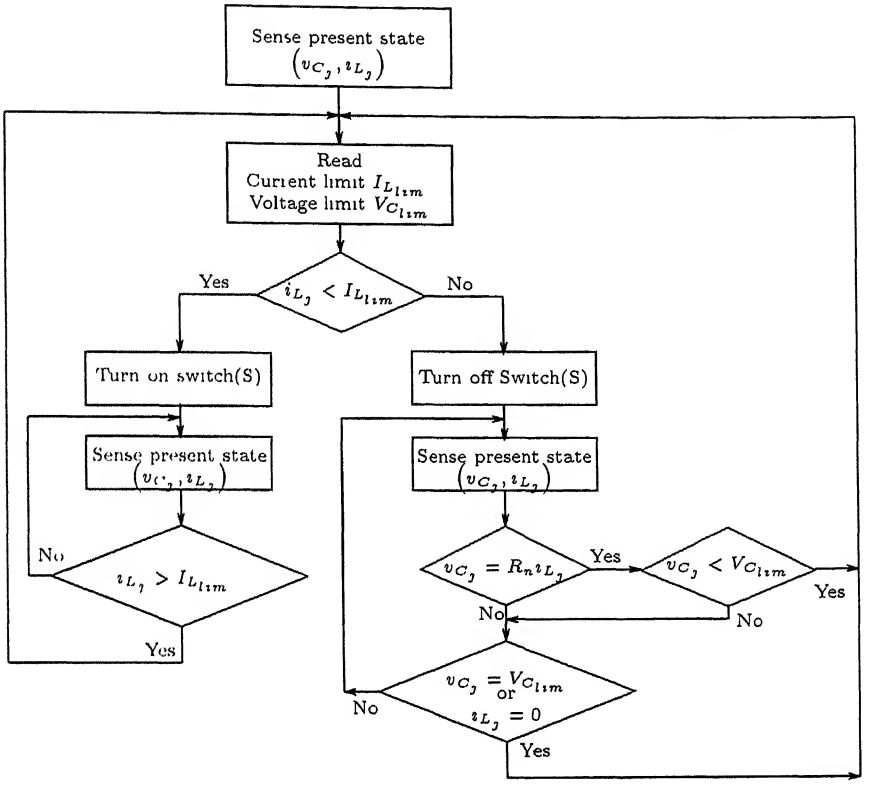

Figure 4.1: Logic required to generate the switching sequence for $I_{in}\&V_{out}$ controller

Region III :- $v_{Cn} < V_{Cn_{lim}}$ and $i_{Ln} > I_{Ln_{lim}}$

Region IV :- $v_{Cn} > V_{Cn_{lim}}$ and $i_{Ln} > I_{Ln_{lim}}$

If the initial state of the converter lies in the *region I or II* (as shown by points S or S' in figure 4.2(A)), the power switch will be *turned on.* The inductor current will start increasing, and system states will move along the path SA or S'A', which are the segements of the *on time trajectory* through point S or S'. The switch on interval, will be allowed to continue till the time inductor current is less than $I_{Ln_{lim}}$. The switch will be turned off when the inductor current is equal to $I_{Ln_{lim}}$. The capacitor voltage will start increasing(or decreasing for A'), and the system state will follow the off time trajectory through A or A', i. e. segments AB or A'B'. The switch off interval will be maintained till capacitor voltage becomes $V_{Cn_{lim}}$, i. e. point B or B'.

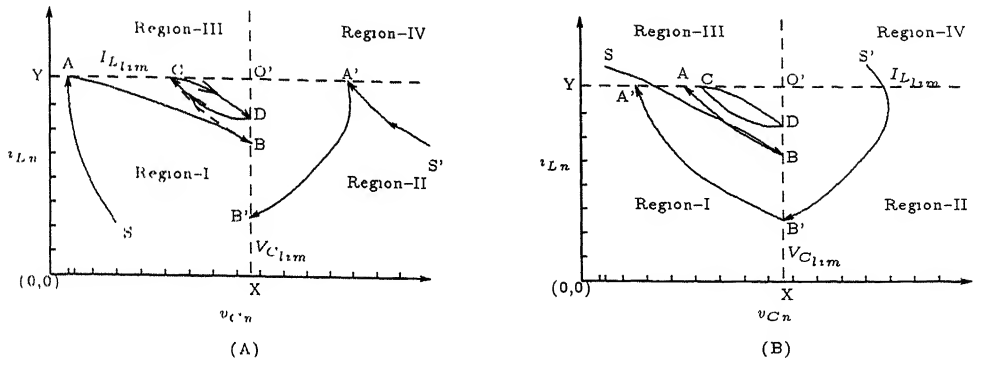

Figure 4.2: The various regions of converter operation with I_{in}&V_{out} controller

At this point of time the switch will be turned on again and the next cycle will be continued.

If the initial state of the converter lies in the *region III or IV* as shown by point S or S' in figure 4.2(B), the power switch will be *turned off* at the start. The system state will move along segments SB or S'B', till capacitor voltage reaches $V_{Cn_{lim}}$ A switch will be turned on then and system states will advance along path BA or B'A. This on time interval will be terminated at point A or A' where inductor current becomes equal to $I_{Ln_{lim}}$. Thus the next cycle will be started at point A or A'.

It can also be seen from the figure 4.2 that with this controller the inductor current and capacitor voltage can be bought within the specified limit, after one cycle of transient operation, irrespective of the initial state of the converter. The further operation will take place, keeping the inductor current and capacitor voltage below specified limit. As a result the system will attain the steady state cycle CDC or C'D'C' as shown in figure 4.2 .

The Special Cases of Converter Operating with I_{in}&V_{out} Controller

To understand the various conditions used in logical diagram (figure 4.1) we will study the special cases of converter operating with this controller.

Case 1:- Consider the initial state of the converter in region III as shown by point S in the figure 4.3. As explained above the switch will be turned off and system state will move along the off time trajectory passing through S, i. e. curve SA in figure4.3. At point A the capacitor voltage will be equal to $V_{Cn_{lim}}$. However it can be seen that at this point the inductor current is greater than $I_{Ln_{lim}}$. If the switch is turned on at this point, the system state will move along on time trajectory (AA'). As a result the inductor current will further increase. Thus the on time interval will be continued and controller will fail.

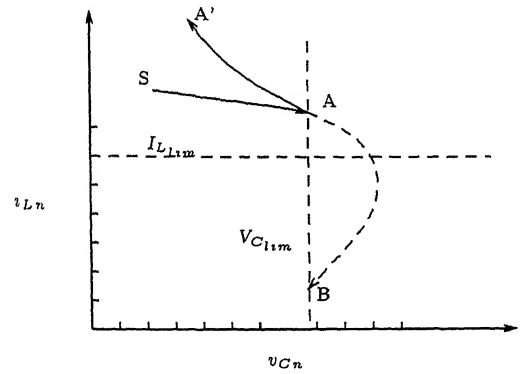

Figure 4.3: Build of i_{Ln} due to faulse turn on of switch

This problem can be avoided, if the switch is allowed to be turned on only when inductor current is less than $I_{Ln_{lim}}$. It shuld be noted that this fact is implemented in logic diagram (figure 4.1) by checking the condition $i_{Ln} < I_{Ln_{lim}}$, before issuing the switch on or switch off commond. Thus in such cases the converter system will be allowed to continue the off time interval till point B . The system state will move along the curve AB as shown in figure4.3.

Case-2:- Consider the initial condition in region IV as shown in figure 4.4. The converter will have a switch off interval at start which can be represented by segment SAB of the off time trajectory. It can be seen that at point B, the inductor current will become zero. If the off time interval is continued further

the converter state will move along the v_{Cn} axis till capacitor voltage reaches $V_{Cn_{lim}}$ (i. e. point C). However if the converter is required to operate in the continuous current conduction mode of operation the off time interval should be terminated at point B. The system states will then move along the path BB' (a portion of on time trajectory).

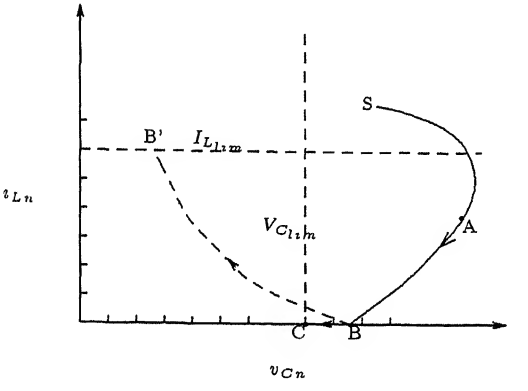

Figure 4.4: A disontinuous current conduction mode of converter operation under I_{in}&V_{out} controller

In the logic diagram(figure4.1) the condition $i_{Ln} = 0$ is checked during off time interval to avoid the discontinous mode of operation.

Case 3:- This controller needs the two reference quantities namely *inductor current and capacitor voltage limits.* Although these two quantities are independent if they are specified seperately the resultant system may have a slow transient response in some cases as shown in figure 4.5. The peak voltages of the *off time trajectories* passing through point A_1&A_2 are less than the set voltage limit($V_{Cn_{lim}}$). Hence each time the off time interval will be continued till boundary point(B_1&B_2). Thus the time taken to achive the required steady state is large.

This problem can be overcome if the switch off interval is terminated at the peak voltage point if it occurs before the capacitor voltage reaches the limit.

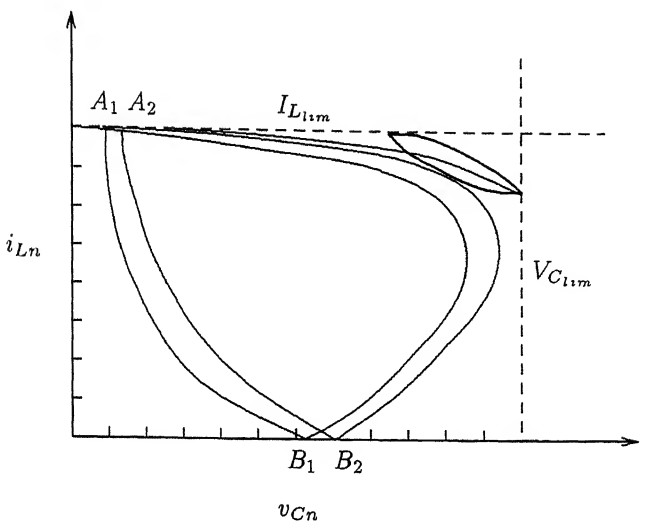

Figure 4.5: A slow response case of the converter operation under $I_{in}\&V_{out}$ controller

Thus the sensing of peak voltage point is also required to generate the switching sequence. It can be vary easily implemented by using equation 2.56 as shown in figure 4.1.

4.1.2 The Simulation of the Controller

The response of the converter has been simulated with the help of the algorithm given in figure 4.6. The results are obtained by computer program based on this algorithm using the MATLAB package.

The results shown in figures 4.7 to 4.10 are generated for the converter having $R_n = 0.7$ and input voltage =1 p. u. . The initial states of the converter has been selected from the each of the four regions as explained in section 4.1.1. The voltage and current limits are selected by trial and error method to obtain the average output voltage equal to one. It has be seen from the simulated results that for the converter operation in high frequency low ripple region, the average output voltage can be approximated as $V_{Cn_{lim}}$. In such cases the variation in current limit results in variation of output voltage ripple. It should be noted that in such cases the

selection of voltage limit can also be done with the help of the performance curves obtained in chapter 3(figures 3.3 to 3.9).

Further it can be seen from the simulation results that for the fixed value of the voltage and current limits, a unique steady state is achived irrespective of the initial condition of the converter.

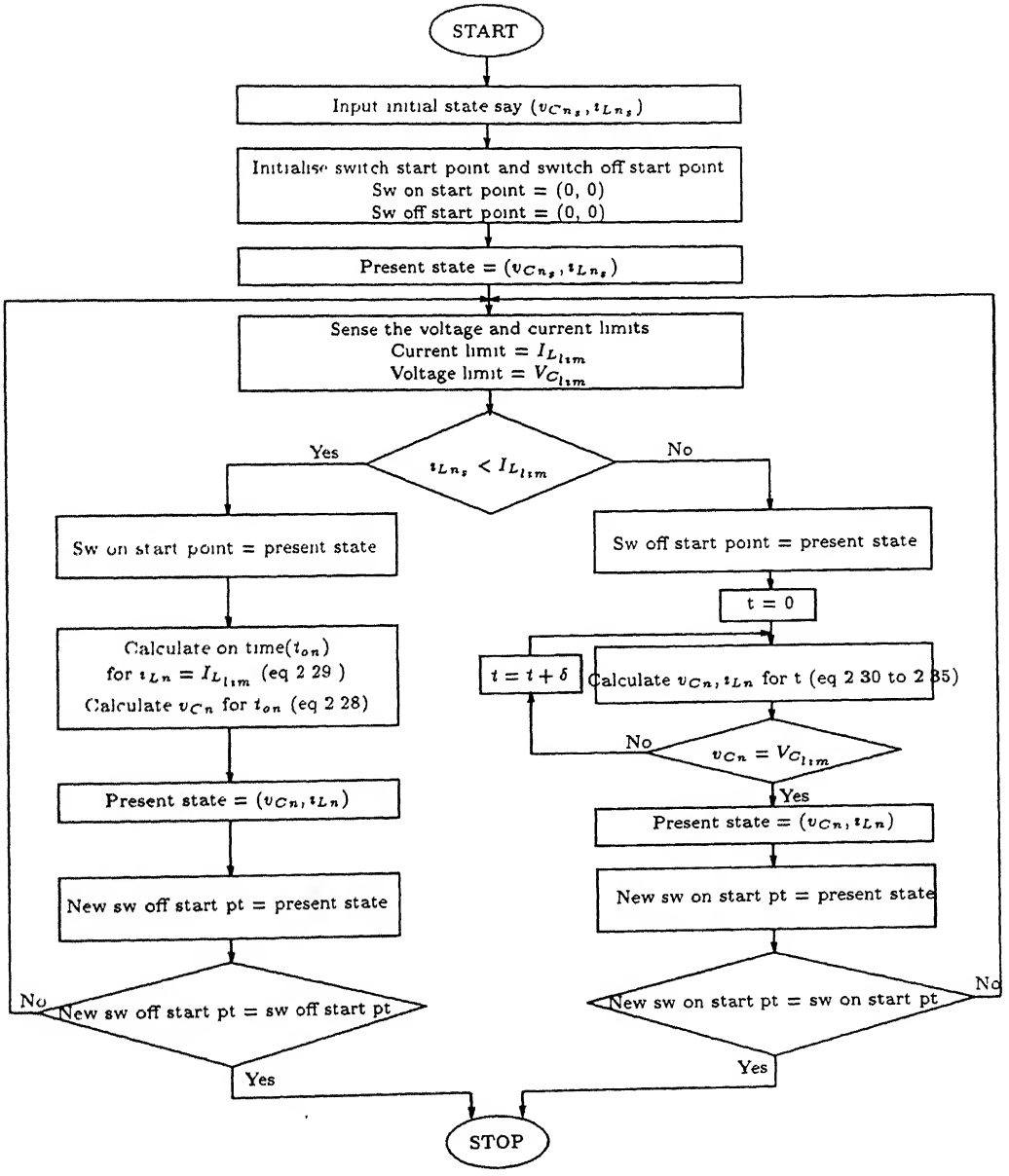

Figure 4.6: The flow chart for simulation of converter operation with $I_{in}\&V_{out}$ controller

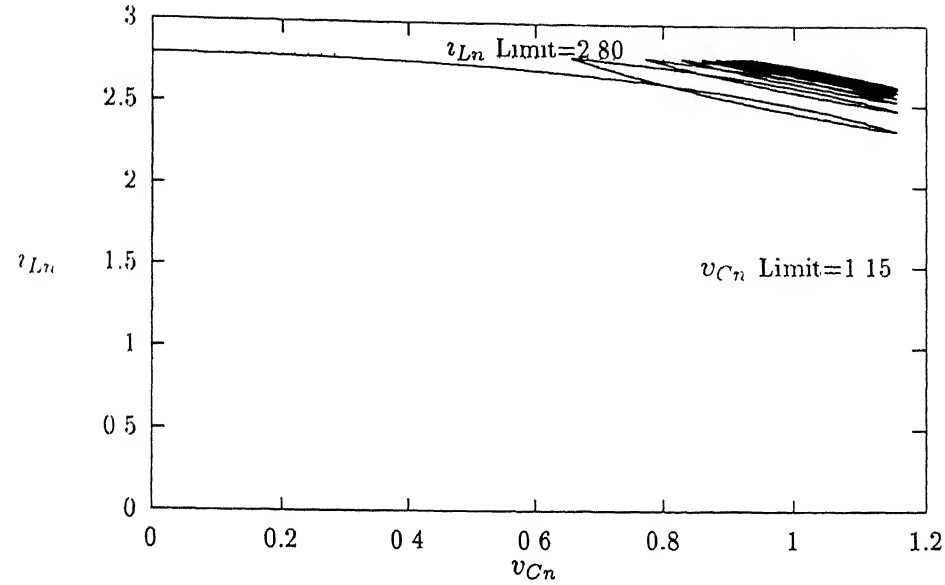

Initial State = (0,0)

Figure 4.7: Simulated responce of the 'I_{in}&V_{out} *controller*' for the converter with initial condition in region I

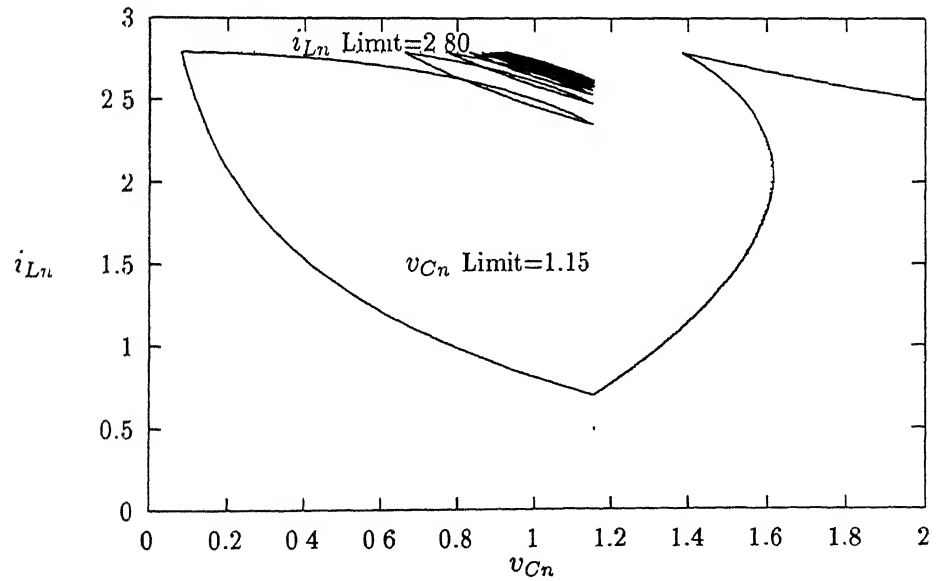

Initial State = (2,2.5)

Figure 4.8: Simulated responce of the 'I_{in}&V_{out} *controller*' for the converter with initial condition in region II

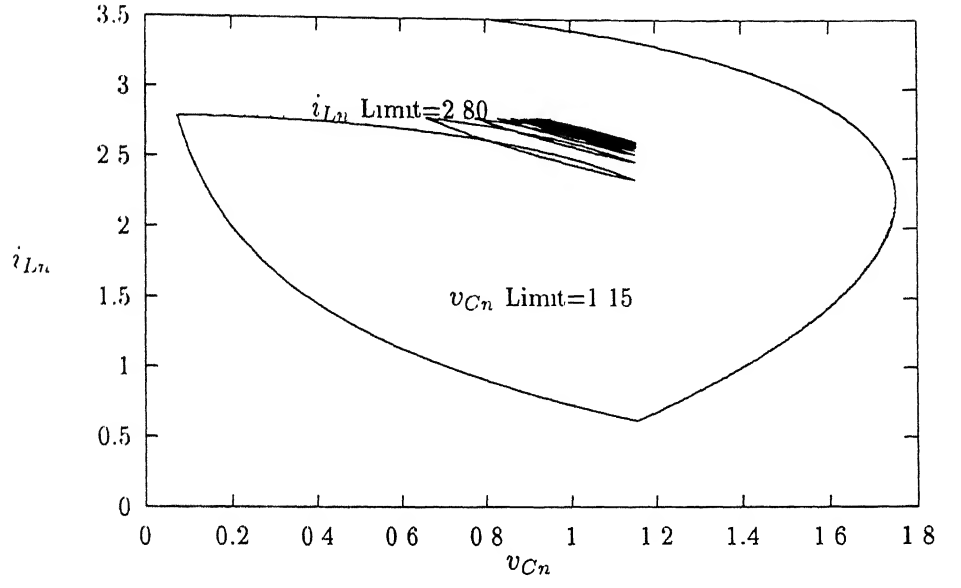

Initial State = (0.8,3.5)

Figure 4.9: Simulated responce of the 'I_{in}&V_{out} *controller*' for the converter with initial condition in region III

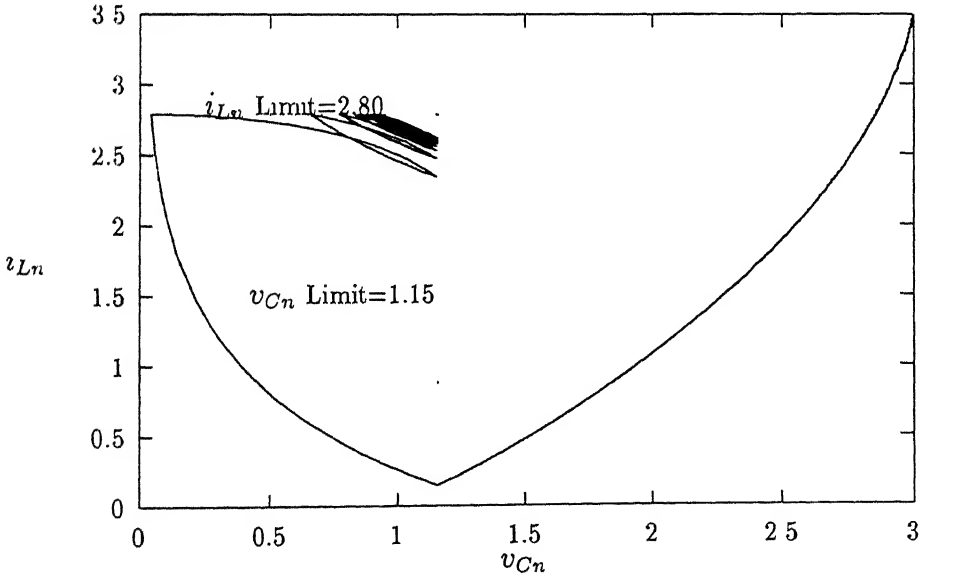

Initial State = (3,3.5)

Figure 4.10: Simulated responce of the 'I_{in}&V_{out} *controller*' for the converter with initial condition in region IV

4.2 Energy Level Controller

As shown in appendix C, the normlized stored energy in a converter system is given by the following expression

$$\begin{aligned} \text{Total Normalized Stored Energy}(SE_n) &= i_{Ln}^2(t) + v_{Cn}^2(t) \\ &= \text{the square of the magnitude of the} \\ &\quad \text{polar vector describing state trajectories} \end{aligned}$$

Thus the various states of the converter at which the stored energy is constant, must lie on a circle. The figures 4.11(A) & 4.11(B) show the variation of the total stored energy during *on time interval* and *off time interval* respectively. It can

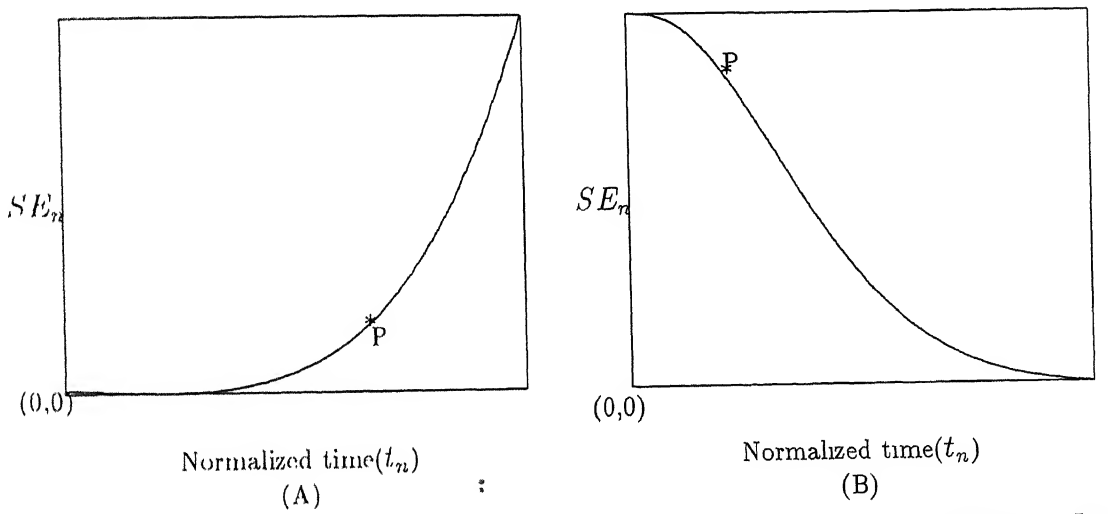

Figure 4.11: The variation in SE_n during *On time interval* and *Off Time Interval*

be seen from these figures that the total stored energy of the converter system monotonically increases during on time interval and monotonically decreases during off time interval. Hence this quantity(SE_n) can be used to control the state of the power switch. The converter can then be made to operate between the specified band of energy(i. e. between the two limits of energy).

In most of the practical cases the desired stored energy levels of the converter are not specified. This poses the major problem in selection of the energy band when

the controller is to be designed from the set of the specified parameters/variables. However if the desired output voltage ripple is low(below 5%) the selection of the energy band can be done as discussed below.

As explained in section 2.6.5, the low ripple steady state operation of the converter takes place in the vicinity of the tangent point of the constituting off time trajectory and the average state of such steady state operation can be approximated as this tangent point. Further it can be seen from figure 4.11 that the variation in the stored energy can also be approximated as the liner variation in the vicinity of the tangent point P. Hence the stored energy corresponding to the average state of the steady state cycle can be given by the following expression.

$$\begin{bmatrix}\text{Energy corresponding to the}\\ \text{average state of steady state}\\ \text{operation}\end{bmatrix} = \frac{1}{2}\begin{bmatrix}\text{Sum of the stored energy}\\ \text{corresponding to the two}\\ \text{corner states of the steady}\\ \text{state operation}\end{bmatrix} \tag{4.1}$$

From the above discussion it can be concluded that for a high normalized frequency and low ripple operation of converter, the selection of the energy band can be done such that the mean of the two stored energy limits is equal to the stored energy of the average state for the desired steady state operation and the width of the band can be varied to meet the ripple requirment. The detail procedure is explained in the following paragraph.

Consider the the low ripple high frequency operation of the converter as shown in figure 4.12. The two corner points of this operation are shown as points A and B. The *constant stored energy circle* corresponding to the stored energy of these corner states are shown as A'AA" and B'BB" respectively.The average state of this steady state operation is represented by a point O. Let the specified values of the average output voltage and average output current be $V_{O_{av}}$ and $I_{O_{av}}$ respectively. The selection of the stored energy limits can be done with the help of the flow chart given in figure 4.13.

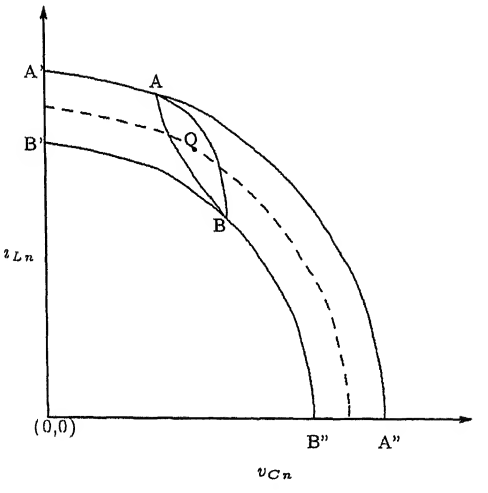

Figure 4.12: A steady state operation within a stored energy band

It should be noted that the frequency of operation and duty ratio is not explicitely controlled in this technique.

4.2.1 Action of the Controller

The switching sequence can be generated by the logic digaram shown in figure 4.14. The power switch is turned on if the total stored energy of the converter system is below the specified upper limit and turned off otherwise.

4.2.2 The Simulation Of Energy Orbit Controller

The simulation of the converter has been carried out using computer program based on the algorithm given in figure 4.14. The simulated respose of the converter having $R_n = 0.8$ & initial condition (0,0), is shown in figure 4.15. The selection of the energy band is done so as to have average output voltage($V_{O_{av}}$) unity and output voltage ripple 5%. The values of upper limit and lower limit of stored energy are calculated as shown in figure 4.13. For the better understanding the steady state operation region(i. e. the region marked with the square box in figure 4.15) has been

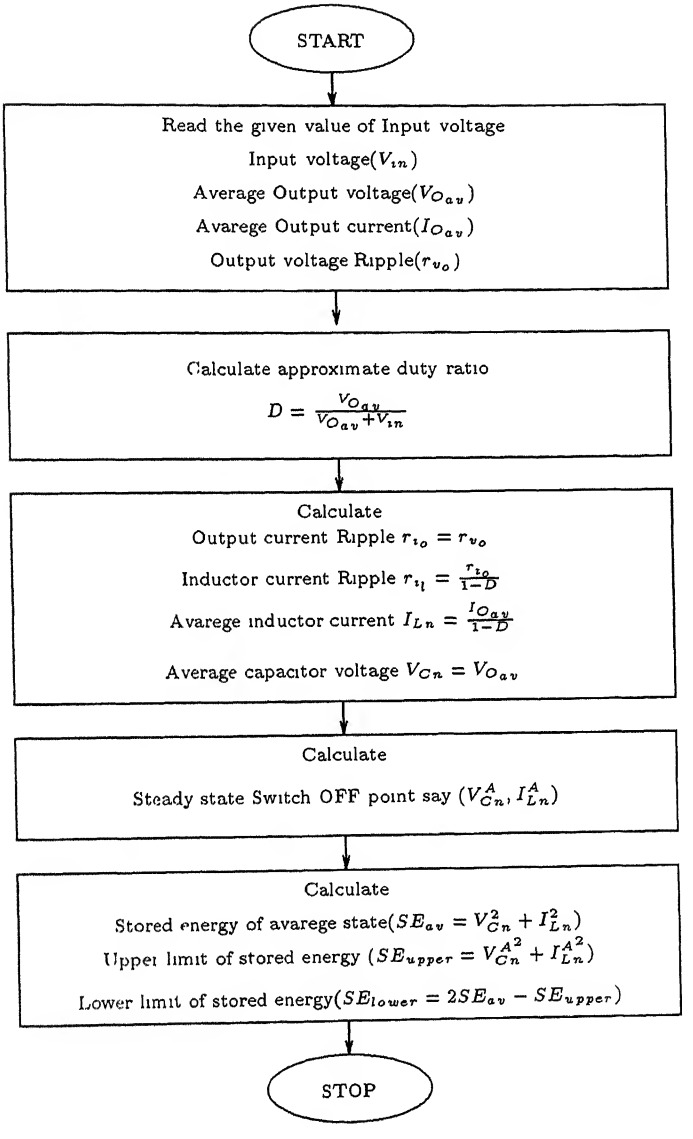

Figure 4.13: Flow chart for selection of the energy band

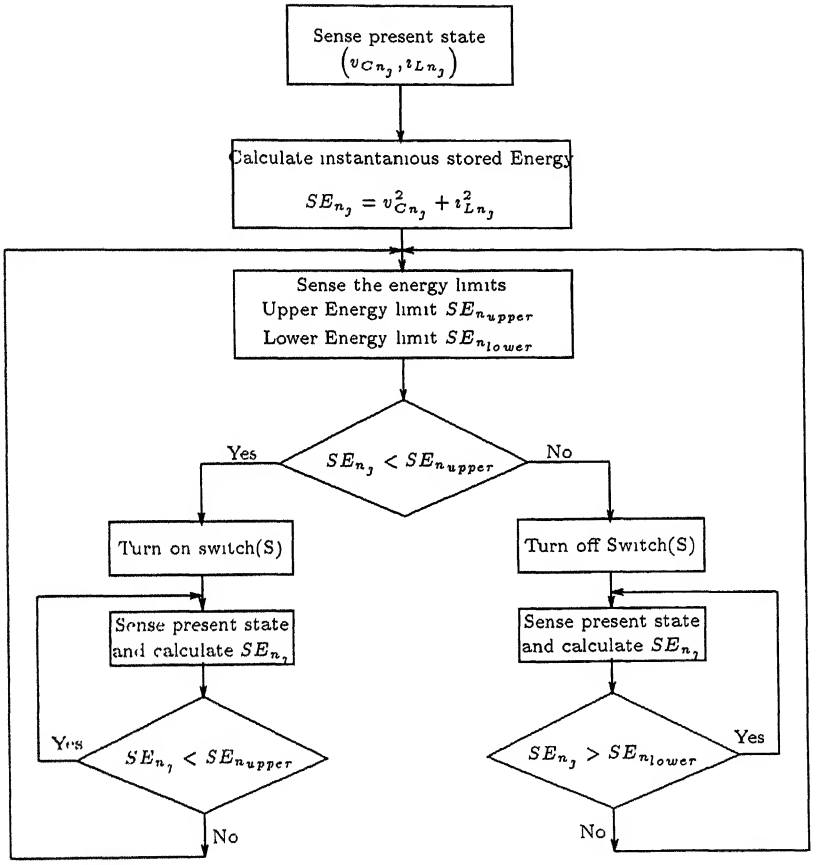

Figure 4.14: Logic required to generate the switching sequence for Energy level controller

enlarged and shown in figure 4.16.

In figure 4.17 the width of the energy band has been varied to study the effect on the output voltage. It can be seen from this figure that the ripple in the output voltage increases with increase in width of energy band.

The figures 4.18 & 4.19 shows the response of the converter for various values of initial conditions. It can be seen from these figures that, if the converter is made to operate in a fixed stored energy band, the unique steady state is achived irrespective of the initial condition of the converter.

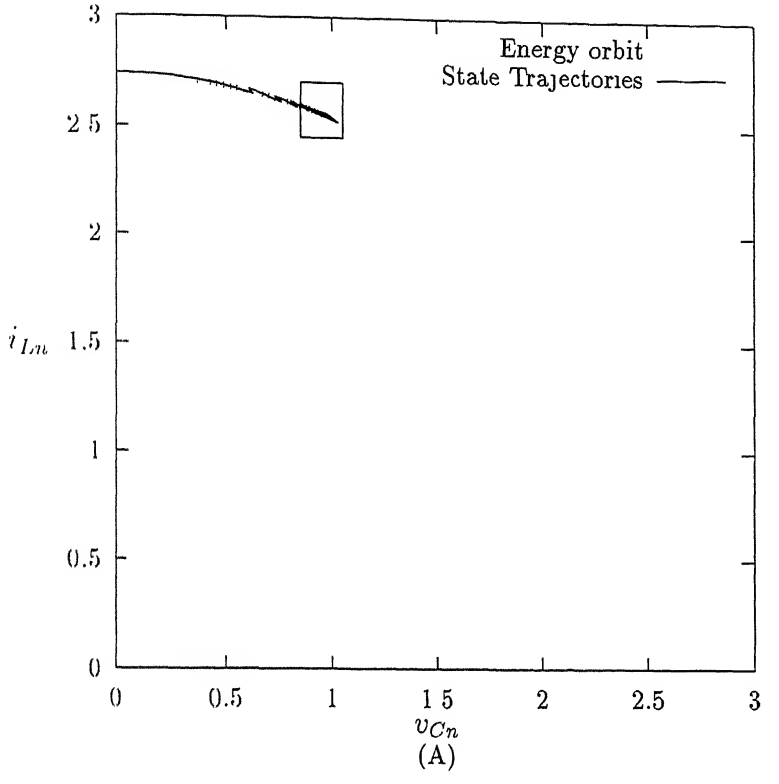

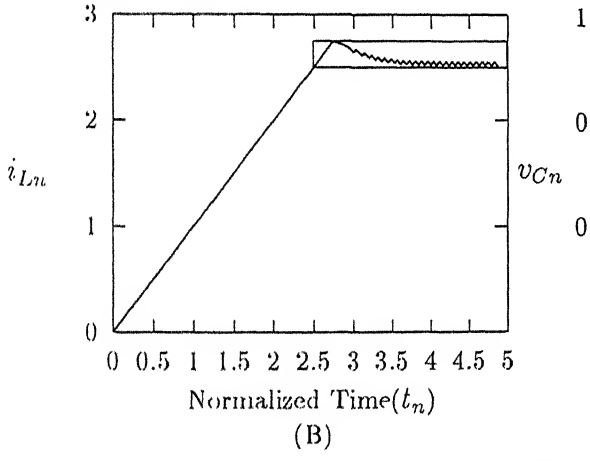

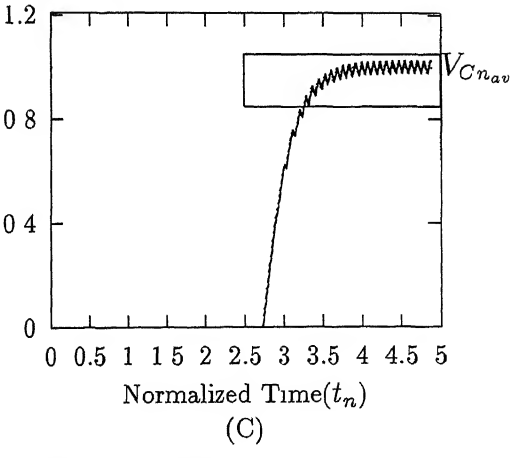

Initial State = (0,0)

Upper Energy Limit = 7.5

Lower Energy Limit = 7.4

Figure 4.15: The simulation of energy level controller for low ripple operation

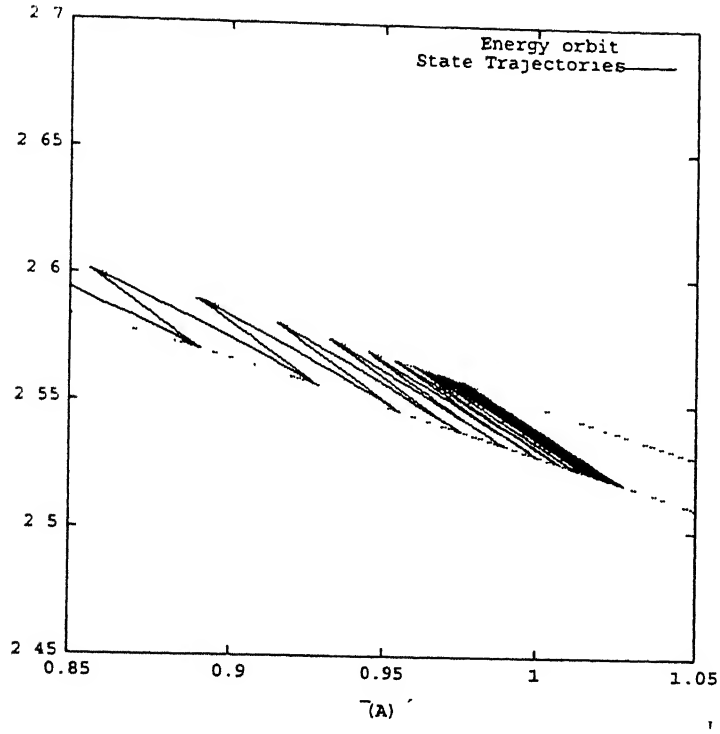

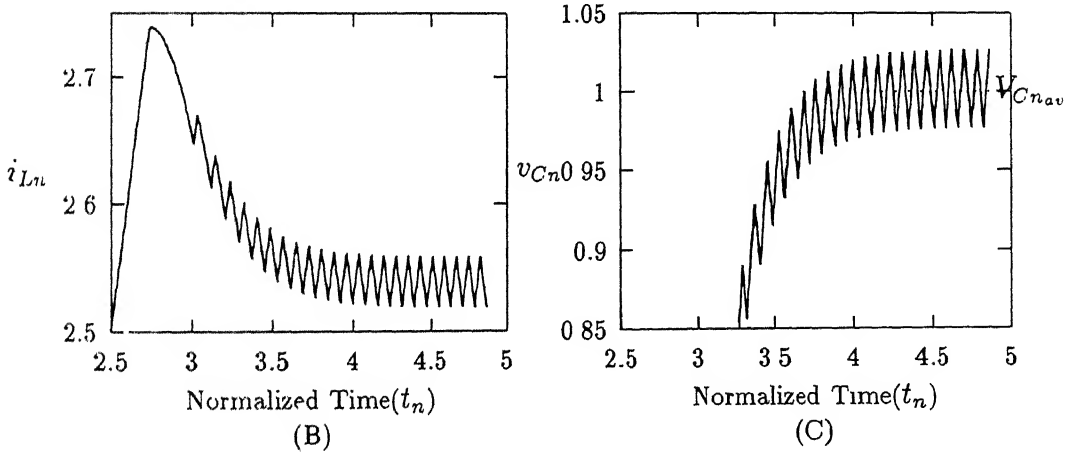

Initial State = (0,0)

Upper Energy Limit = 7.5

Lower Energy Limit = 7.4

Figure 4.16: The simulation results in steady state region

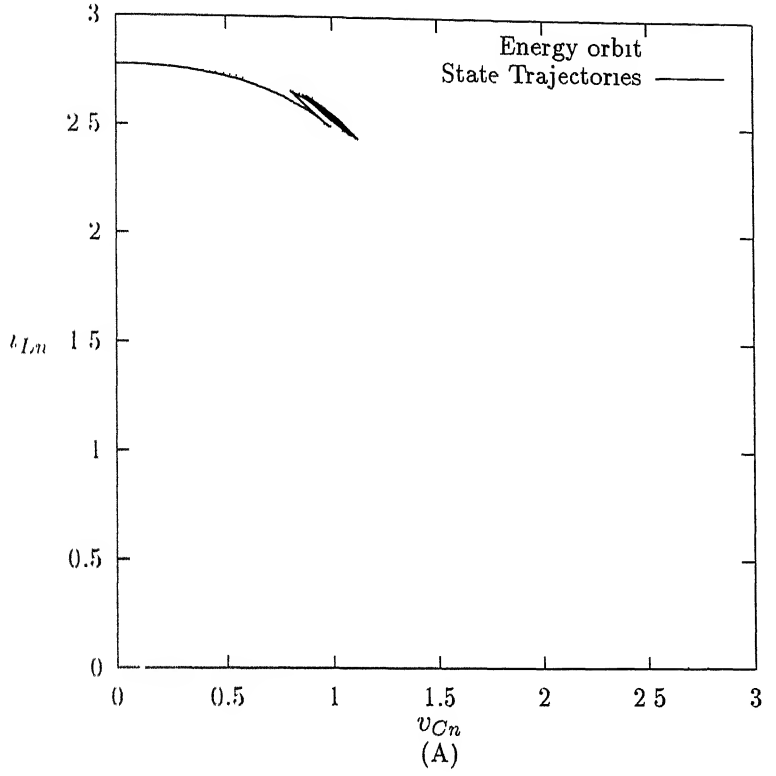

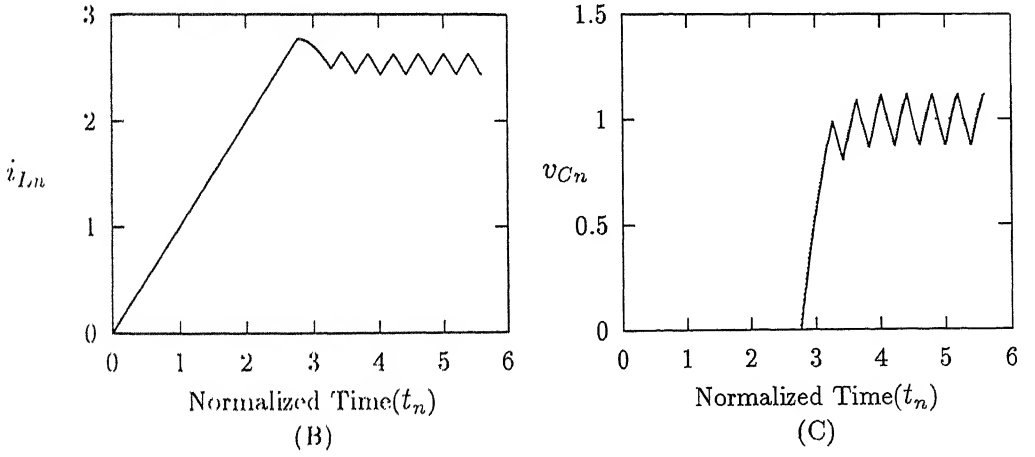

Initial State = (0,0)

Upper Energy Limit = 7.7

Lower Energy Limit = 7.2

Figure 4.17: The simulation showing effect of variation in width of the energy band

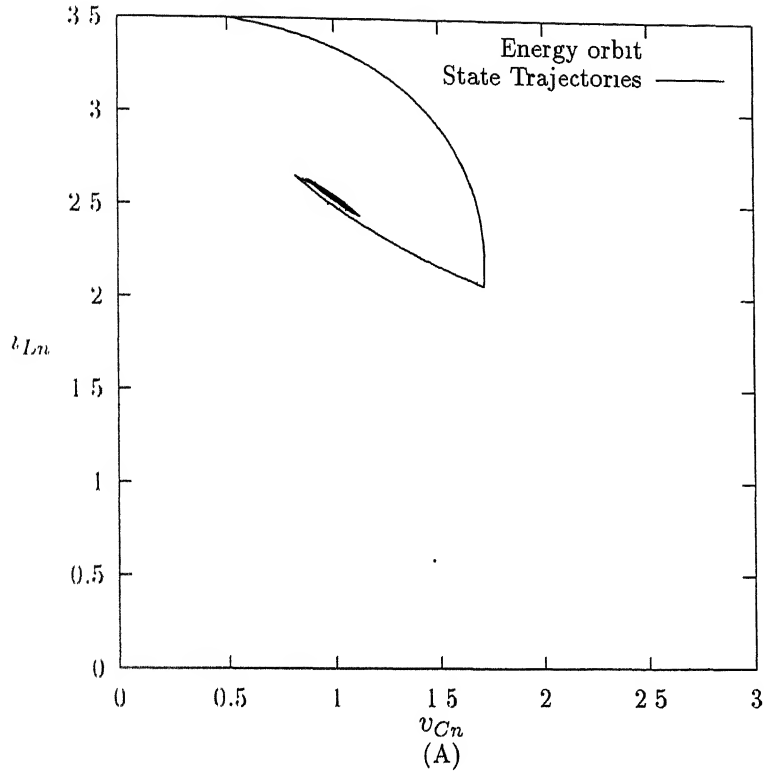

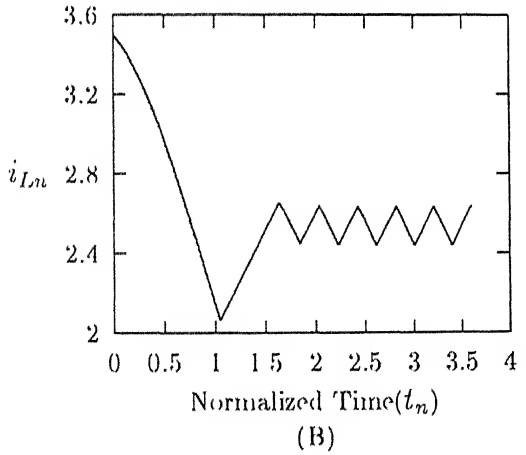

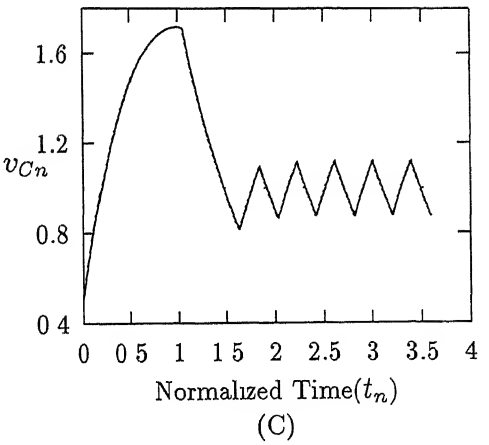

Initial State = (0.5,3.5)

Upper Energy Limit = 7.7

Lower Energy Limit = 7.2

Figure 4.18: The simulation of converter with initial condition lying out side the upper energy limit

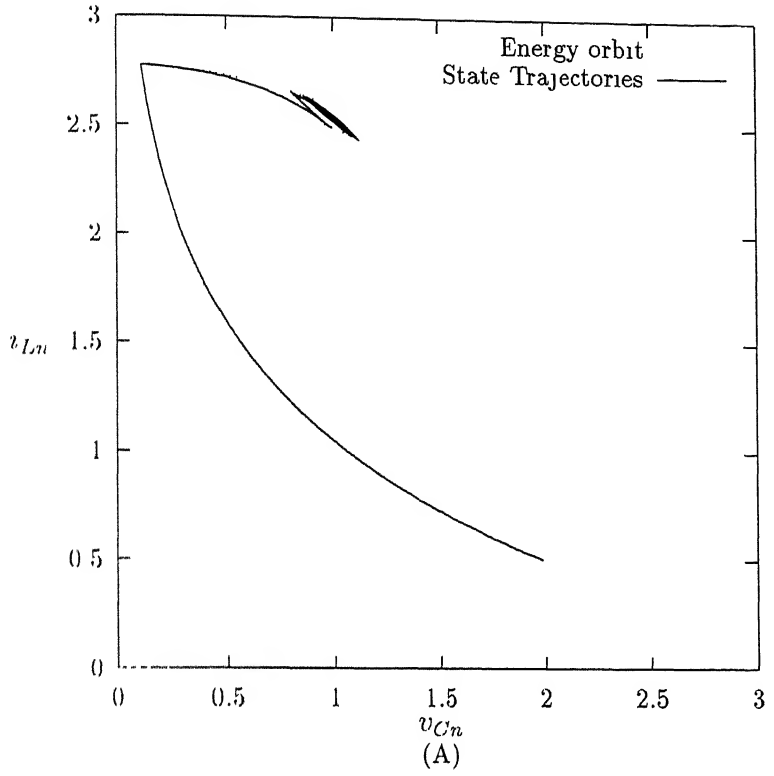

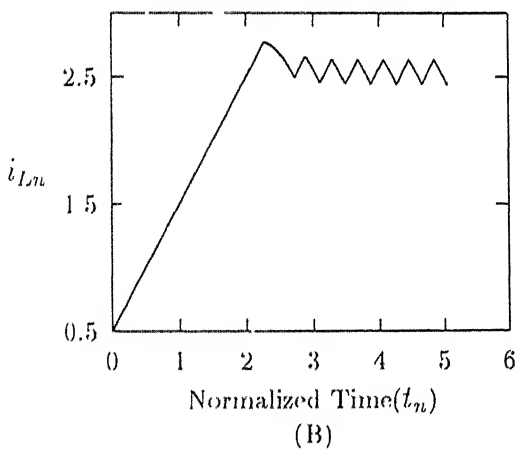

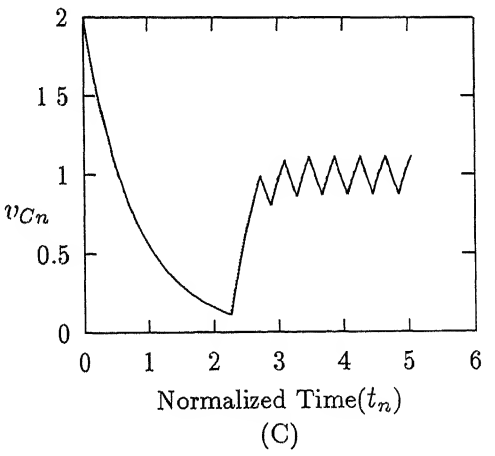

Initial State = (2,0.5)

Upper Energy Limit = 7.7

Lower Energy Limit = 7.2

Figure 4.19: The simulation of converter with initial condition lying inside the u
energy limit

4.3 State Trajectory Control law

It has been shown in chapter 2 that for a fixed values of *source voltage and load resistance* there exists a unique steady state operation which yields a unique average output voltage and current. No other closed trajectory in the state plane yields exactly the same output. The *on time trajectory* and *off time trajectory* which comprises the unique desired steady state cycle can be used as a boundary to divide the state plane into the *switch on region* and *switch off region.*

The figure 4.20(A) shows a steady state operation AB_2BB_1A. The on time trajectory($O'BB_1A$) and off time trajectory(OAB_2B) comprising this steady state cycle are shown with solid line and broken line repectively. With the help of these trajectories, the *switch on region* and *switch off region.* of the state plane can be defined as shown in figure 4.20(B). In this figure the curve OAB_1BO' divides the state plane into two parts. The area below this curve is the defined as *Switch On Region* and area above this curve is defined as *Switch Off region.* The portion of the off time trajectory(i. e. curve OA, including point A) is considered to be the part of the switch off region. Similarly the portion of the on time trajectory(i. e. curve AB_1BO', excluding the point A) is considered to be the part of the switch on region. It should be noted that, it is possiable to use section AB_2B instead of AB_1B. However the later is more convenient for implementation purpose and hence will be used in this chapter.

4.3.1 The Action of the Controller

The control law can be made such that, the power switch is *turned on* whenever the system state is in the on region and *turned off* otherwise. Thus the converter can be brought to the desired steady state trajectory in one *on/off* cycle of control, regardless of the initial condition(state of system). Any change in operating condition i e. the change in source voltage or change in load resistance is immediately reflected as a change in the shape or location of state trajectories. Hence the switching bound-

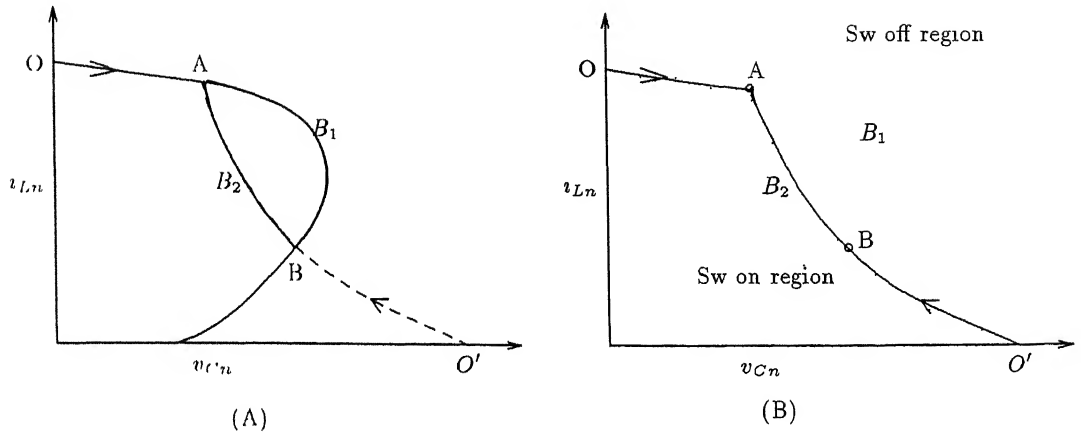

Figure 4.20: The defination of the switching boundary

ary and consequently the switching sequence issued by controller is also changed. This sensitivity to change in the operating condition enables the controller to locate the unique desired steady state trajectory for all operating conditions.

This controller is a free running in the sense that during transient condition, it permits the power switch to remain open or closed for as long as it is needed to accomplish the necessary redistribution of energy in the converter power stage, in order to attain desired output. But at the same time, it enables the constant frequrncy or constant duty ratio operation in steady state, if desired.

4.3.2 Implementation of Trajectory Control Law

Construction of The Switching Boundary

As explained in section 2.6.3 the unique steady state operation and the contituting state trajectories can be specified by specifying any one of the corner points of steady state operation cycle. However during discontinuous current conduction operation, the steady state switch on point lies on v_{Cn} axis. In such cases the predection of the exact off time trajectory is not possible with the help of this point. Thus the *steady state switch off point* is a convenient choice for specifing both the trajectories.

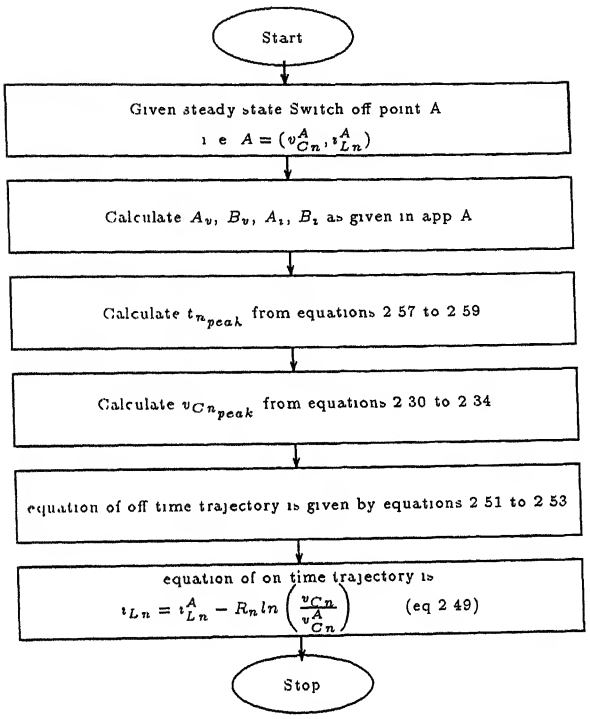

Figure 4.21: The Procedure for finding the equations of trajectories defining the switching boundary

If the duty ratio(D) and the the operation time(T_n) is known the exact location of the equilibrium switch off point can be determined from equations 2.42 to 2.44. However it should be noted that, if the converter is operating in high frequency, low ripple region, the *steady state switch off point* can be approximately determined from the value of the average output voltage and output ripple. The algorithm given in figure 4.13 can be used for determining the co-ordinates of tthe steady state switch offf point. Having determined the coordinates of the steady state switch off point the switching boundary(i. e. curve OAB_2BO' in figure 4.20) can be constructed by selecting the *off time trajectory* and the *on time trajectory* passing through this point. The equations of these trajectories can be written with the help of a flow chart given in figure 4.21.

Generation of Switching Sequence

Once the switching boundary is defined mathematically, the formulation of the associated switch on/off region and the generation of the switching sequence can be done as shown by a logic diagram in figure 4.22.

Results of simulation

The various converter operations have been simulated by using the computer program based on above logic diagram. The results given in figure 4.23 to 4.25 shows the simulated operation of the converter having following data

- Required average output voltage = 0.5 p.u
- Output voltage ripple = 5%
- Per unit load resistance = 0.9

The initial conditions are selected arbitrary. The figures A shows the state space picture of the converter operation, whereas the figures (B) & (C) s gives the time domain response. It can be seen from these figures that the converter attains the desired steady state in one cycle of switching.

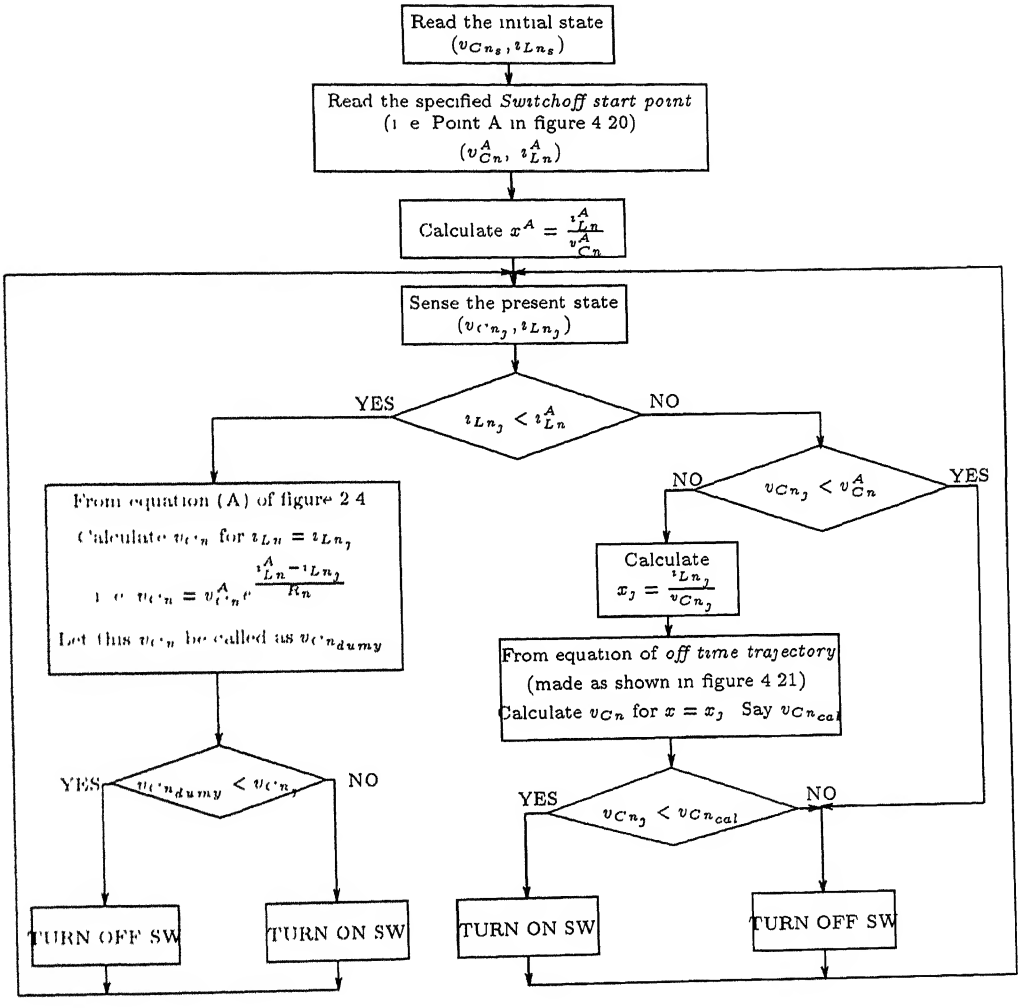

Figure 4.22: Logic required for generating the switching sequence for trajectory law controller

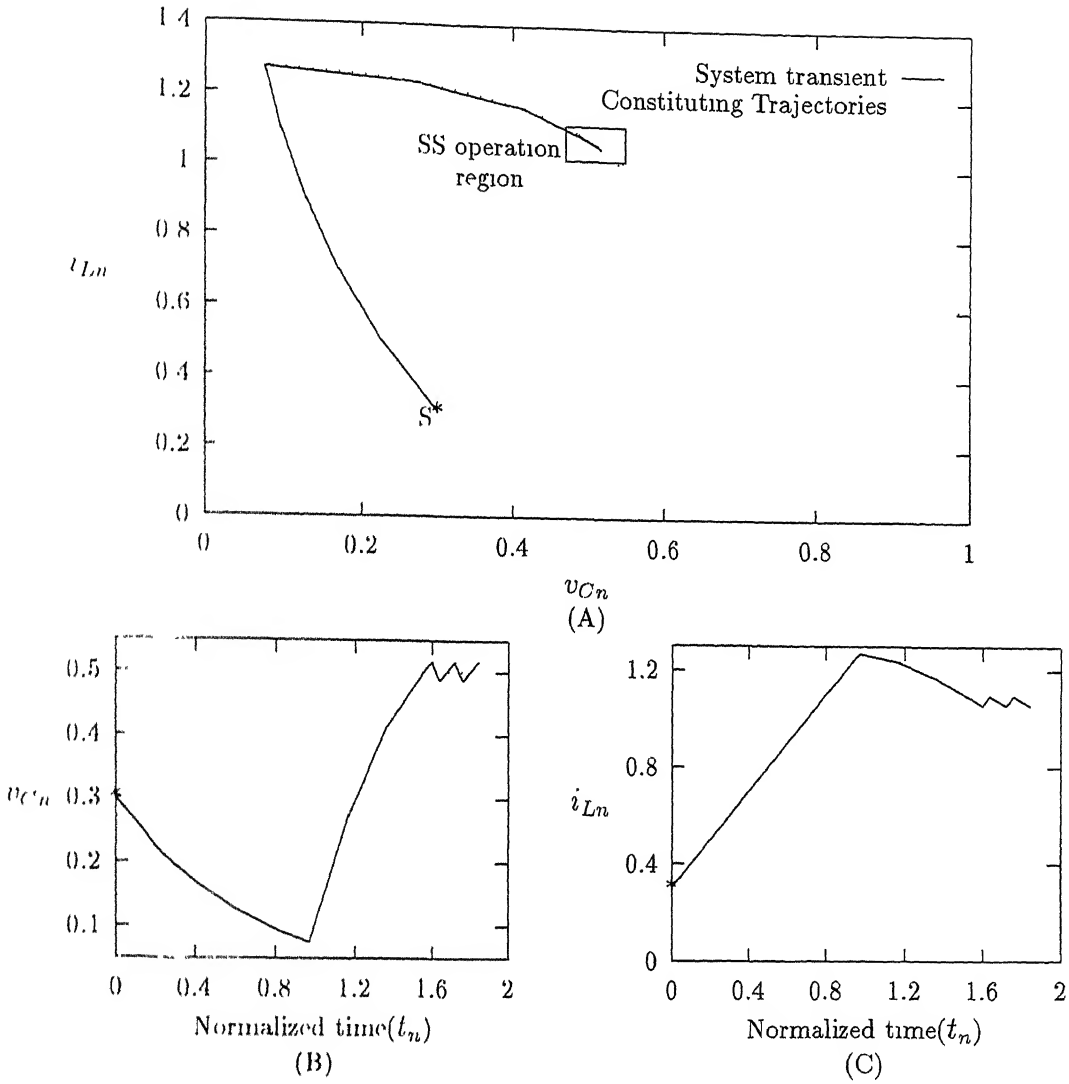

Initial State = (0.3,0.3)

Desired Average output voltage = 0.5 p. u.

Desired output voltage ripple = 5%

Figure 4.23: The simulation of trajectory law controller with initial condition (0.3,0.3)

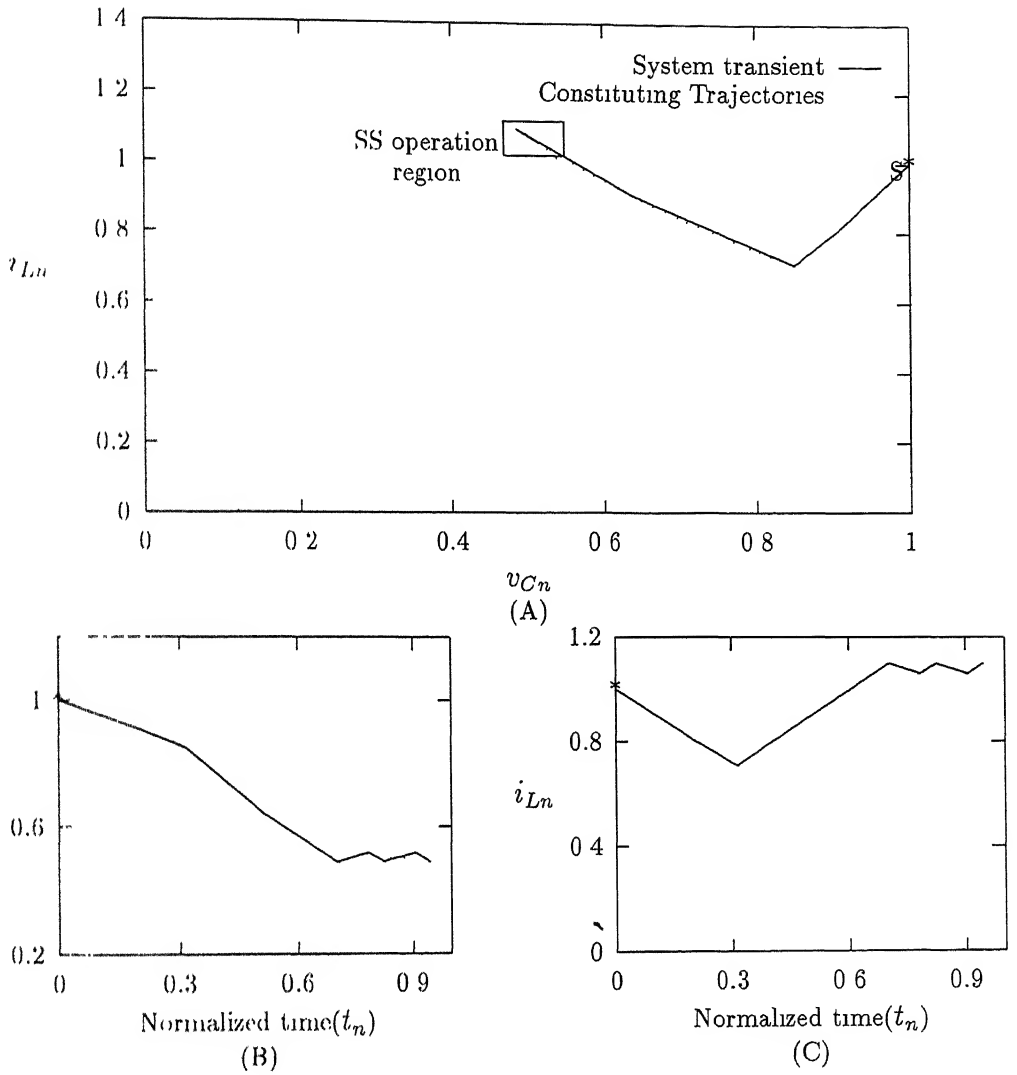

Initial State = (1,1)

Desired Average output voltage = 0.5 p. u.

Desired output voltage ripple = 5%

Figure 4.24: The simulation of trajectory law controller with initial condition (1,1)

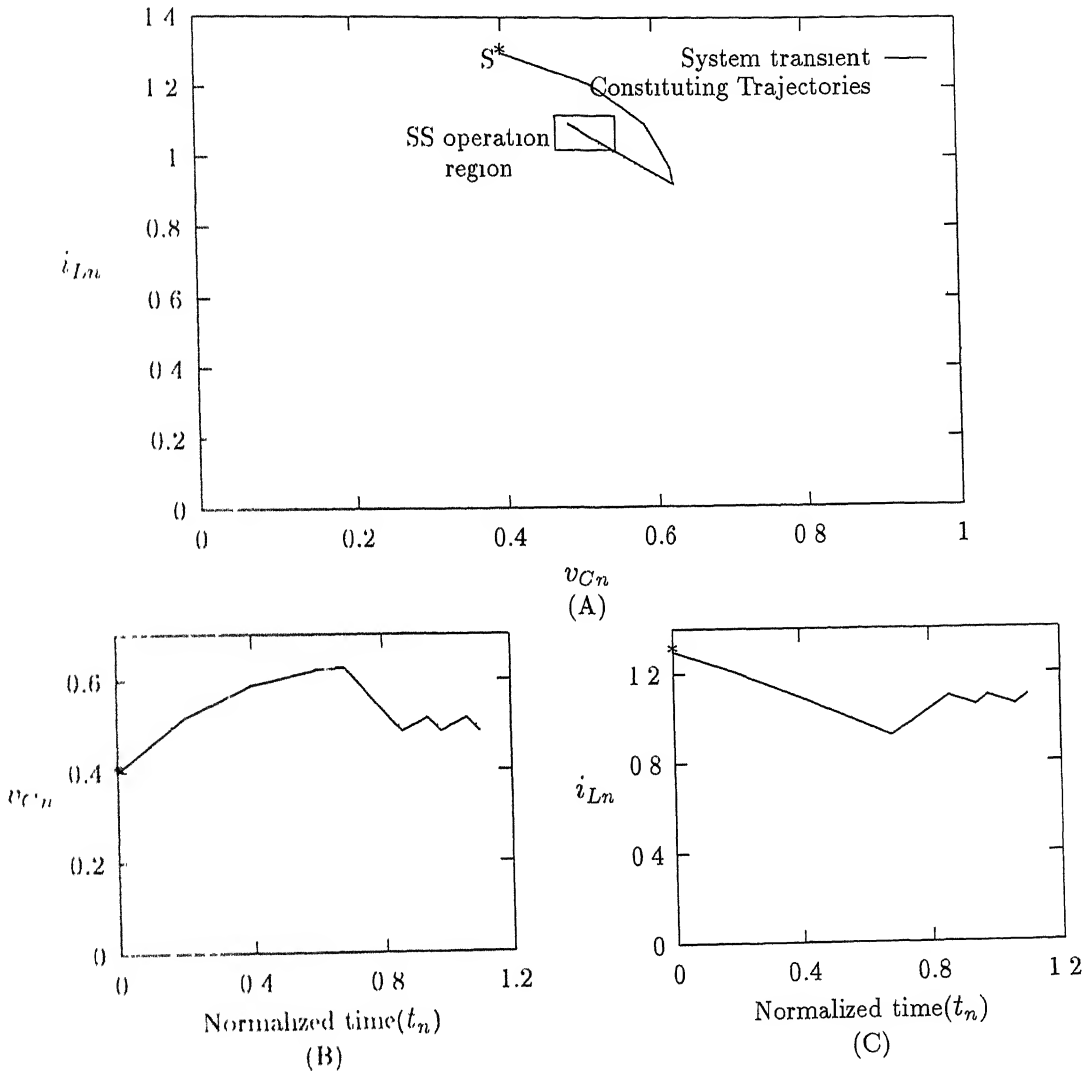

Initial State = (0.4,1.3)

Desired Average output voltage = 0.5 p. u.

Desired output voltage ripple = 5%

Figure 4.25: The simulation of trajectory law controller with initial condition (0.4,1.3)

4.4 Conclusions

The converter operation under following control strategies has been simulated

- Input current limit and output voltage limit control
- Stored energy level control
- Trajectory law control

The converter reaches a fixed steady state under all three strategies, starting from different operating points. The converter operation under the third strategy, attains the desired steady state in one operating cycle. however this controller is a complex and require a microcomputer based system for implementation. The first two controllers are simpler to make but takes more time to reach a desired steady state.

Chapter 5

Conclusion

The general qualitative investigation of Buck Boost dc-to-dc converter, has been presented in this thesis. The state plane analysis approach, employed in this investigation, reveals the families of state trajectories which system state must follow during switch off time and switch on time as a result of system governing law. The use of these independent state trajectories has been shown to be a valuable method for analysis of the converter.

In chapter 2 an analytic equation, each for on time trajectory and off time trajectory has been obtained apart from normal time domain solution. The expression for off time trajectory involves the slope($\frac{i_{Ln}}{v_{Cn}}$) of the polar vector describing the off time trajectory as a parameter. These expressions allow direct on line determination of the state trajectory.

Further the well known analysis, neglecting the ripple in v_C & i_L (appendix D) has been correlated to the state trajectories, in the form of a tangent point. The off time trajectory has been shown to have a distinct peak in capacitor voltage. This peak point lies along the stright line having slope of $1/R_n$.

The performance curves obtained in chapter 3 are in normalized form and can be used for a variety of converter operations. The technique based on these performance curves for designing the values of inductor and capacitor has been suggested. It has been shown that a per unit resistance of value in the range of 2-2.5 at the rated

operating point results in an optimal values of inductor and capacitor. A higher value of per unit resistance, increases the value of capacitor without resulting the significant reduction in value of inductor.

It has been shown with the help of performance curves that a steady state operation at higher values of *per unit load resistance* results in lowering the *switching frequency*, for a given value of *percentage ripple*. The study of the performance curve in *high normalised frequency region* show that the average output voltage and duty ratio are independent of operation time in this region.

The operation of the converter under three different control strategies has been studied in chapter 4. These strategies are as follows

- Input current limit and output voltage limit controller
- Stored energy level controller
- Trajectory law controller

The first two strategies employ limits on variables or energy to generate the switching sequence. However in the third strategy, the equations of state trajectories constituting the unique required steady state are used as a boundry for switching on or off. In all these strategies the operating frequency and duty ratio are not explicitly controlled. It has been shown with the help of simulated response that, the converter running under the *trajectory control law* achieves the required steady state operation in one switching(on/off) cycle

5.1 Recommendations for Future Work

- A more detailed model of converter using series resistence of inductor (L) and capacitor (C) can be simulated to obtain more accurate performance curve at chapter 3.

- These curves have been obtained for continuous current conduction mode of converter operation. They can be extended to include the discontinuous conduction mode of operation.

- The method of designing the values of inductor and capacitor can be modified to include the cost of L and C as factor deciding the exact value of L and C. The most economical values of L and C can be obtained by this method.

- The response of different controllers in chapter 4 can be compared to bring out the relative marits and demerits.

- The practical implementation of the trajectory law controller can be carried out.

Bibliography

[1] W. W. Burns, III, and T. G. Wilson, "*State trajectories used to observe and control dc to dc converter*," IEEE Trans. Aerosp. Electron. Syst., Vol. AES-12, No. 6, pp. 706 717, Nov. 1976.

[2] W. W. Burns, III, and T. G. Wilson, "*A state-trajectory control law for dc–to–dc converters*," IEEE Trans. Aerosp. Electron. Syst., Vol. AES-14, No.-1, pp. 1 20, Jan. 1978.

[3] N. Mohan, T. M. Undeland, and W. P. Robbins, "*Power electronics: converters, applications, and design*," John Wiley, 1994.

[4] D. M. Mitchell, "*DC' DC' Switching regulator analysis*," McGraw-Hill, 1988.

[5] '*MATLAB:User's guide*', The Math Work Inc., 1993.

Appendix A

Time Domain Solution of State Equations During Off Time Interval

The state equation during switch off period are

$$\frac{dv_{cn}}{dt_n} = -\frac{v_{cn}}{R_n} + i_{Ln} \tag{A.1}$$

$$\frac{di_{Ln}}{dt_n} = -v_{cn} \tag{A.2}$$

The time domain solution can be obtained by separating the variables i_{Ln} and v_{cn} from above equations. Thus the equations obtained by separating the variables are

$$\frac{d^2v_{cn}}{dt_n^2} + \frac{1}{R_n}\frac{dv_{cn}}{dt_n} + v_{cn} = 0 \tag{A.3}$$

$$\frac{d^2i_{Ln}}{dt_n^2} + \frac{1}{R_n}\frac{di_{Ln}}{dt_n} + i_{Ln} = 0 \tag{A.4}$$

The charactristic eqation of these differential eqations can be written as

$$s^2 + a_1 s + a_2 = 0 \quad \text{where} \quad a_1 = \frac{1}{R_n} \ , a_2 = 1$$

The roots of charateristic eqation are

$$s_1, s_2 = -\frac{a_1}{2} \pm \sqrt{\left(\frac{a_1}{2}\right)^2 - 1}$$

These roots have three possible forms, depending upon the quantity $\left(\frac{a_1^2}{2} - 1\right)$. Hence the solution also will have three forms as shown in the table below

Case	Condition	Nature of Roots	Descriptive Name	Form of Solution
1	$a_1^2 > 4a_2$	real and unequal	over damped	$k_1 e^{s_1 t} + k_2 e^{s_2 t}$
2	$a_1^2 = 4a_2$	real and equal	critically damped	$(k_1 + k_2 t)e^{s_1 t}$
3	$a_1^2 < 4a_2$	complex conjugate	under damped	$e^{\sigma t}(k_1 cos(\omega t) + k_2 sin(\omega t))$ where, σ = real(s_1) and ω = imaginary(s_1)

Where k_1 and k_2 are integration constants and can be calculated from knowledge of initial conditions of variable.

Let the initial condition of the converter at the start of switch off interval be $((v_{Cn}^0)_{off}, (i_{Ln}^0)_{off})$. Thus the solution of equations (A.3) and (A.4) and the values of the intigration constants can be written as follows

Case 1 ($R_n < 1/2$)

$$v_{Cn} = A_v e^{s_1 t_n} + B_v e^{s_2 t_n} \tag{A.5}$$

$$i_{Ln} = A_i e^{s_1 t_n} + B_i e^{s_2 t_n} \tag{A.6}$$

Where

$$A_v = \frac{1}{(s_1 - s_2)}\left[(i_{Ln}^0)_{off} - (v_{Cn}^0)_{off}\left(\frac{1}{R_n} + s_2\right)\right]$$

$$B_v \quad {}_{(s_2 - s_1)}^{1} \left[(i^0_{Ln})_{off} - (v^0_{Cn})_{off} (\tfrac{1}{R_n} + s_1) \right]$$

$$A_i \quad {}_{(s_2 - s_1)}^{1} \left[(v^0_{Cn})_{off} + s_2 (i^0_{Ln})_{off} \right]$$

$$B_i \quad {}_{(s_1 - s_2)}^{1} \left[(v^0_{Cn})_{off} + s_1 (i^0_{Ln})_{off} \right]$$

Case 2 (R_n 1/2)

$$v_{Cn} \quad (A_v + B_v t) e^{s_1 t} \tag{A.7}$$

$$i_{Ln} \quad (A_i + B_i t) e^{s_1 t} \tag{A.8}$$

Where

$$A_v \quad (v^0_{Cn})_{off}$$

$$B_v \quad (v^0_{Cn})_{off} (1 \quad {}^{1}_{R_n}) + (i^0_{Ln})_{off}$$

$$A_i \quad (i^0_{Ln})_{off}$$

$$B_i \quad (i^0_{Ln})_{off} + (v^0_{Cn})_{off}$$

Case 3 (R_n - 1/2)

$$v_{Cn} \quad e^{\sigma t_n} (A_v cos(\omega t_n) + B_v sin(\omega t_n)) \tag{A.9}$$

$$i_{Ln} \quad e^{\sigma t_n} (A_i cos(\omega t_n) + B_i sin(\omega t_n)) \tag{A.10}$$

Where

$$A_v \quad (v^0_{Cn})_{off}$$

$$B_v \quad {}^{1}_{\omega} ((i^0_{Ln})_{off} + (v^0_{Cn})_{off} \sigma)$$

$$A_i \quad (i^0_{Ln})_{off}$$

$$B_i \quad {}^{1}_{\omega} ((v^0_{Cn})_{off} + \sigma (i^0_{Ln})_{off})$$

Appendix B

The Analytic Equation of Off Time Trajectory

The explicit relationships between between v_{Cn} and i_{Ln}, obtained from state equations during off time is

$$\begin{matrix} di_{Ln} & & R_n v_{Cn} \\ dv_{Cn} & (v_{Cn} & R_n i_{Ln}) \end{matrix} \tag{B.1}$$

The solution of equation B.1 can be obtained by using substitution

$$i_{Ln} \quad x v_{Cn} \tag{B.2}$$

By diffrentiating equation B.2, we get

$$\begin{matrix} di_{Ln} \\ dv_{Cn} \end{matrix} \quad x + v_{Cn} \frac{dx}{dv_{Cn}} \tag{B.3}$$

Substituting equation (B.2) and (B.3) in (B.1) we get

$$x + v_{Cn} \frac{dx}{dv_{Cn}} = \frac{R_n v_{Cn}}{v_{Cn} - R_n x v_{Cn}}$$

if $v_{Cn} \neq 0$ we can write

$$x + v_{Cn} \frac{dx}{dv_{Cn}} = \frac{R_n}{1 - R_n x}$$

therefore

$$\frac{dv_{cn}}{v_{cn}} = -\left(\frac{R_n x - 1}{R_n x^2 - x + R_n}\right) dx \tag{B.4}$$

$$= \underbrace{-\frac{1}{2}\left(\frac{2R_n x - 1}{R_n x^2 - x + R_n}\right) dx}_{p} + \underbrace{\frac{1}{2R_n}\left(\frac{1}{R_n x^2 - \frac{1}{R_n} x + 1}\right) dx}_{q} \tag{B.5}$$

The solution of equation (B.5) can be written as

$$ln(v_{cn}) = \int p dx - \frac{1}{2R_n}\int q dx + C \tag{B.6}$$

where C is the constant of integration.

- The first term i.e $\int p dx$ is of the form $\int \frac{dy}{y}$. Hence the solution of first term is

$$\int p dx = -\frac{1}{2} ln(R_n x^2 - x + R_n) \tag{B.7}$$

- The solution of the second term can be obtained by rearranging the denominator. However the denominator has to be rearranged in three different forms depending upon the value of R_n such as

1. For $R_n < 1/2$

$$\int q dx = \int \frac{1}{\left(x - \frac{1}{2R_n}\right)^2 - A^2} dx \tag{B.8}$$

where $A = \frac{\sqrt{1-4R_n^2}}{2R_n}$

Therefore solution of second term in this case is

$$\int q dx = \frac{1}{2A} ln\left(\frac{2R_n x - 1 - 2R_n A}{2R_n x - 1 + 2R_n A}\right) \tag{B.9}$$

2. For $R_n = 1/2$

$$\int q dx = \int \frac{1}{(x-1)^2} dx$$

Hence the solution can be given as

$$\int q dx = -\frac{1}{(x-1)} \tag{B.10}$$

3. For $R_n > 1/2$

$$\int q dx = \int \frac{1}{x - \frac{1}{2R_n} + A^2} dx$$

where $A = \frac{\sqrt{4R_n^2 - 1}}{2R_n}$

Hence solution is

$$\begin{aligned} \int q dx &= \frac{1}{A} tan^{-1}\left(\frac{x - \frac{1}{2R_n}}{A}\right) \\ &= \frac{1}{A} tan^{-1}\left(\frac{2R_n x - 1}{2R_n A}\right) \end{aligned} \tag{B.11}$$

Thus the solution of equation B.1 can be written from equations B.6 through B.11 as follows

- For $R_n < 1/2$

$$ln(v_{Cn}) = -\frac{1}{2} ln(R_n x^2 - x + R_n) + \frac{1}{4R_n A} ln\left(\frac{2R_n x - 1 - 2R_n A}{2R_n x - 1 + 2R_n A}\right) + C \tag{B.12}$$

- For $R_n = 1/2$

$$ln(v_{Cn}) = -ln(x - 1) + \frac{1}{x + 1} + ln(\sqrt{2}) + C \tag{B.13}$$

- For $R_n > 1/2$

$$ln(v_{Cn}) = -\frac{1}{2} ln(R_n x^2 - x + R_n) + \frac{1}{2R_n A} tan^{-1}\left(\frac{2R_n x - 1}{2R_n A}\right) + C \tag{B.14}$$

To calculate the value of constant 'C', the knowledge of a converter state during off time interval is required. The converter state along i_{Ln} axis of state space can not be used for this purpose, since these equations are obtained from assumption that $v_{Cn} \neq 0$,as stated above .

It can be seen from equation B.1 that

when $v_{Cn} = R_n i_{Ln}$

$$\frac{dv_{Cn}}{di_{ln}} = 0$$

This implies that the off time trajectory will have a peak capacitor voltage when v_{c_n} $R_n i_{Ln}$. Hence condition that can be employed to calculate C,is

$$v_{c_n} \quad v_{c_{peak}} \quad \text{at} \quad x = \frac{1}{R_n} \tag{B.15}$$

Thus the equation for off time trajectory can be given as

- *For* R_n · 1/2

$$\ln\left(\frac{v_{c_n}}{v_{c_{peak}}}\right) \quad \frac{1}{2}\ln\left(x^2 - \frac{x}{R_n} + 1\right) + \frac{1}{4R_nA}\ln\left(\frac{(2R_nx - 1 - 2R_nA)(1 + 2R_nA)}{(2R_nx - 1 + 2R_nA)(1 - 2R_nA)}\right) \tag{B.16}$$

.....

Where

$$x \quad \frac{i_{Ln}}{v_{c_n}}$$

& A $\sqrt{\frac{1}{4R_n^2} \cdot 1}$

- *For* R_n 1/2

$$\ln\left(\frac{v_{c_n}}{v_{c_{peak}}}\right) \quad \ln(x-1) + \frac{1}{x-1} - 1 \tag{B.17}$$

- *For* R_n · 1/2

$$\ln\left(\frac{v_{c_n}}{v_{c_{peak}}}\right) \quad \frac{1}{2}\ln\left(x^2 - \frac{x}{R_n} + 1\right) + \frac{1}{2R_nA}\left[\tan^{-1}\left(\frac{2R_nx - 1}{2R_nA}\right) - \tan^{-1}\left(\frac{1}{2R_nA}\right)\right] \tag{B.18}$$

.....

Where

$$x = \frac{i_{Ln}}{v_{c_n}}$$

& $A = \sqrt{1 - \frac{1}{4R_n^2}}$

Appendix C

Expression for the Normalised Stored Energy

The total stored energy in a converter system is given by

$$E_{ts} = \frac{1}{2}Li_L^2 + \frac{1}{2}Cv_C^2 \tag{C.1}$$

$$= \frac{1}{2}L\left(i_{Ln}V_{dc}\sqrt{C/L}\right)^2 + \frac{1}{2}C\left(v_{Cn}V_{dc}\right)^2$$

$$= \frac{1}{2}CV_{dc}^2\left(i_{Ln}^2 + v_{Cn}^2\right) \tag{C.2}$$

Let the base stored energy be defined as

$$E_b = \frac{1}{2}CV_{dc}^2$$

Thus the normalised stored energy of the converter can be given as

$$E_{tn} = \frac{E_{tn}}{E_b} = i_{Ln}^2 + v_{Cn}^2) \tag{C.3}$$

Appendix D

Analysis of converter under low ripple, high frequency approximations

For the converter operating at high switching frequency, the variation in inductor current(i_{Ln}) and capacitor voltage(v_{Cn}) can be approximated as a linear variation. The figure D.1 shows a steady state cycle of such operation.

Due to the high switching frequency t_{on} and t_{off} will be very small. Hence the converter behaviour can be described using the following equations

Mode 1 (S_{ON} **and** D_{OFF})

$$\Delta v_{Cn} \approx -\frac{v_{Cn}}{R_n}\Delta t_n = -\frac{v_{Cn}}{R_n}DT_n \tag{D.1}$$

$$\Delta i_{Ln} \approx \Delta t_n = DT_n \tag{D.2}$$

Mode 2 (S_{OFF} **and** D_{ON})

$$\Delta v_{Cn} \approx \left(-\frac{v_{Cn}}{R_n} + i_{Ln}\right)\Delta t_n = \left(-\frac{v_{Cn}}{R_n} + i_{Ln}\right)(1-D)T_n \tag{D.3}$$

$$\Delta i_{Ln} \approx -v_{Cn}\Delta t_n = -v_{Cn}(1-D)T_n \tag{D.4}$$

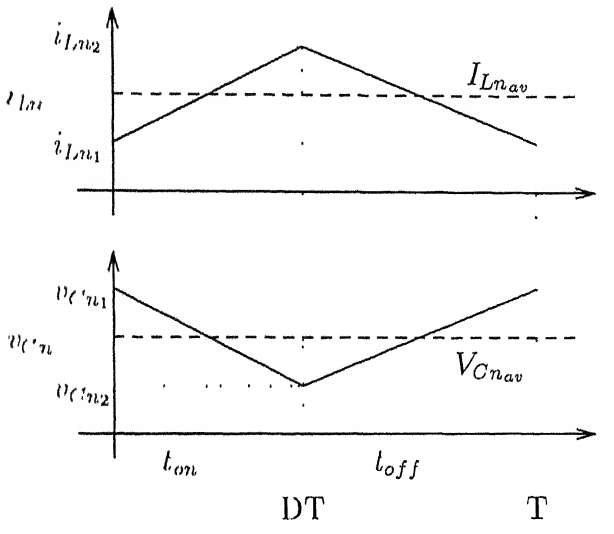

Figure D.1: A steady state operation at high switching frequency

If the capacitor is large we can assume that

$$\begin{aligned} v_{Cn} &\approx V_{Cn_{av}} \\ i_{Ln} &\approx I_{Ln_{av}} \end{aligned} \tag{D.5}$$

During the steady state condition

$$\begin{aligned} |\Delta v_{Cn} \text{of Mode 1}| &= |\Delta v_{Cn} \text{of Mode-2}| \\ |\Delta i_{Ln} \text{of Mode 1}| &= |\Delta i_{Ln} \text{of Mode-2}| \end{aligned} \tag{D.6}$$

Hence from equations D.1, D.3 & D.6, we can write

$$I_{Ln_{av}} = \frac{V_{Cn_{av}}}{R_n} \frac{1}{1-D} \tag{D.7}$$

If the serire resistance of the capacitor is neglected $V_{Cn_{av}} = V_{O_{av}}$ Hence equation D.7 can be written as

$$I_{Ln_{av}} = I_{O_{av}} \frac{1}{1-D} \tag{D.8}$$

Similarly from equations D.2, D.4 & D.6, we can write

$$V_{O_{av}} = \frac{D}{1-D} \tag{D.9}$$